A TRIDENT SCHOLAR
PROJECT REPORT

NO. 152

Prediction of Helicopter Free Flight Trim Using a State of the Art
Analytical Model

UNITED STATES NAVAL ACADEMY
ANNAPOLIS, MARYLAND

88 11 03 002

REPORT DOCUMENTATION PAGE		READ INSTRUCTIONS BEFORE COMPLETING FORM
1. REPORT NUMBER U.S.N.A. - TSPR; no. 152 (1988)	2. GOVT ACCESSION NO.	3. RECIPIENT'S CATALOG NUMBER
4. TITLE *(and Subtitle)* PREDICTION OF HELICOPTER FREE FLIGHT TRIM USING A STATE OF THE ART ANALYTICAL MODEL.		5. TYPE OF REPORT & PERIOD COVERED Final 1977/1988
		6. PERFORMING ORG. REPORT NUMBER
7. AUTHOR(s) Glen W. Pendrick		8. CONTRACT OR GRANT NUMBER(s)
9. PERFORMING ORGANIZATION NAME AND ADDRESS United States Naval Academy, Annapolis.		10. PROGRAM ELEMENT, PROJECT, TASK AREA & WORK UNIT NUMBERS
11. CONTROLLING OFFICE NAME AND ADDRESS United States Naval Academy, Annapolis		12. REPORT DATE 18 July 1988
		13. NUMBER OF PAGES 60
14. MONITORING AGENCY NAME & ADDRESS *(if different from Controlling Office)*		15. SECURITY CLASS. *(of this report)*
		15a. DECLASSIFICATION/DOWNGRADING SCHEDULE

16. DISTRIBUTION STATEMENT *(of this Report)*

This document has been approved for public release; its distribution is
UNLIMITED.

17. DISTRIBUTION STATEMENT *(of the abstract entered in Block 20, if different from Report)*

18. SUPPLEMENTARY NOTES

Accepted by the U.S. Trident Scholar committee.

19. KEY WORDS *(Continue on reverse side if necessary and identify by block number)*

Helicopters
Rotors
Aerodynamics
Numerical analysis .

20. ABSTRACT *(Continue on reverse side if necessary and identify by block number)*

    To aid in the design and analysis of rotors, a reliable and efficient
code of aircraft aerodynamics is required. With such a code, expensive flight
test time may be optimized. A reliable code also allows the engineer to
determine the relationship between full scale wind tunnel tests and free flight.
In this report, the research code CAMRAD, Comprehensive Analytical Model of
Rotocraft Aerodynamics and Dynamics, is investigated to determine if it can be
(OVER)

relied upon to construct a free flight test matrix for the prototype Boeing Vertol Helicopter Model 360. Excellent correlation was found between CAMRAD'S wind tunnel analysis and testing data on the Model 360 in the Duits-Nederlandse Windtunnel (DNW) for forward flight conditions. CAMRAD was unable to properly simulate partial power descent conditions from the DNW. The free flight analysis on CAMRAD compared well to theoretical helicopter aerodynamics. A free flight test matrix was constructed from the CAMRAD simulation.

Accession For

NTIS GRA&I	✓
DTIC TAB	
Unannounced	
Justification	

By
Distribution/

| Availability Codes |
| Avail and/or |
| Dist | Special |

A-1
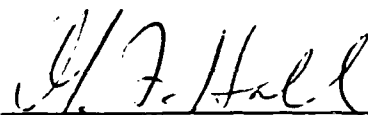
Prediction of Helicopter Free Flight Trim Using a State of the Art Analytical Model

A Trident Scholar Project Report

by
Midshipman Glenn W. Pendrick, Class of 1988
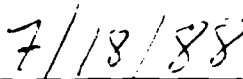U.S. Naval Academy
Annapolis, Maryland

Associate Professor Gerald F. Hall
Aerospace Engineering Department

Accepted for Trident Scholar Committee

Professor D.F. Hasson
Chairperson

7/18/88
Date

USNA-1531-2

ABSTRACT

To aid in the design and analysis of rotors, a reliable and efficient code of aircraft aerodynamics is required. With such a code, expensive flight test time may be optimized. A reliable code also allows the engineer to determine the relationship between full scale wind tunnel tests and free flight. In this report, the research code CAMRAD, Comprehensive Analytical Model of Rotorcraft Aerodynamics and Dynamics, is investigated to determine if it can be relied upon to construct a free flight test matrix for the prototype Boeing Vertol Helicopter Model 360. Excellent correlation was found between CAMRAD's wind tunnel analysis and testing data on the Model 360 in the Duits-Nederlandse Windtunnel (DNW) for forward flight conditions. CAMRAD was unable to properly simulate partial power descent conditions from the DNW. The free flight analysis on CAMRAD compared well to theoretical helicopter aerodynamics. A free flight test matrix was constructed from the CAMRAD simulation.

Preface

At this point, I would like to thank all those who have contributed to the completion of this Trident Scholar Project. Associate Professor Gerald F. Hall of the Aerospace Engineering Department was a tremendous help to me in all aspects and an endless well of knowledge. Mr. Robert Disque of the CADIG Department was a major factor in getting everything accomplished. His computer expertise was always appreciated. And most importantly I would like to thank Alison for providing the support I needed. She always understood.

List of Symbols

Ω Rotor rotational speed (revolutions per minute or radians per second)

$\varnothing$ Wake age, angular positon of wake vortex segment relative to generating blade

ψ Angular position of blade

N   Number of rotor blades

R   Radius of blade, ft

c   Chord of blade, ft

μ Helicopter advance ratio $= V_f/V_{tip}$

q   Freestream dynamic pressure $= \rho v^2/2$, lb/ft^2

a   Sound speed, ft/sec

A   Rotor disc area, πR^2, ft^2

A_b Rotor blade area, NcR, ft^2

σ Solidity, A_b/A

V_f Helicopter forward speed, ft/sec

V_{tip} Rotor tip speed, ΩR, ft/sec

M_{tip} Blade tip Mach number, $\Omega R/a$

C_H Rotor drag force coefficient, $H/\rho A(\Omega R)^2$

C_T Rotor thrust coefficient, $T/\rho A(\Omega R)^2$

C_X Rotor propulsive coefficient, $X/\rho A(\Omega R)^2$

XBAR   Nondimensional propulsive force in wind coordinates, $X/4qR^2$

β_{1c} Longitudinal tip path plane tilt angle, positive forward, degrees

β_{1s} Lateral tip path plane tilt angle, positive toward retreating side, degrees

θ_0 Collective pitch angle, degrees

θ_{1c} Lateral cyclic pitch angle, degrees

θ_{1s} Longitudinal cyclic pitch angle, degrees

v Rotor induced velocity, positive downward, ft/sec

v_h Ideal hover induced velocity, $(T/2\rho A)^{1/2}$, ft/sec

$\bar{v}$ Aircraft control vector, degrees

$\bar{v}_p$ Pilot control vector, degrees

$\bar{v}_o$ Aircraft control vector with all sticks centered, degrees

Table of Contents

I. INTRODUCTION

The aircraft design process can be both time consuming and costly. To actually monitor the exact behavior of a prototype aircraft, it must be flight tested. For state of the art rotors this can require an inordinate amount of wind tunnel testing and flight testing to cover the performance envelope. This is extremely expensive and time consuming. In order to minimize this test time and its associated financial expense in the iterative design process, a numerical analysis that accurately predicts the helicopter performance parameters is a useful design tool. CAMRAD, Comprehensive Analytical Model of Rotorcraft Aerodynamics and Dynamics, is such a state of the art analysis. Because CAMRAD is itself state of the art, its reliability must necessarily be checked as it is utilized for advanced rotorcraft designs. The Boeing Vertol Helicopter Model 360 is an advanced soft rotor system utilizing new composites in its construction. The purpose of this report is to determine if CAMRAD can be relied upon to construct a free flight test matrix for the prototype Boeing Vertol Helicopter Model 360, and to locate boundaries of its applicability, if any.

II. OVERVIEW OF NUMERICAL ANALYSIS

CAMRAD is applicable to a wide range of flight vehicles. In CAMRAD, rotor performance, loading, and noise; helicopter airframe vibration and

gust performance; and flight dynamics and stability are some of the flight parameters that are covered. Variables such as number of blades; number of rotors; articulated, hingeless, and gimballed and teetering rotors are included in CAMRAD. Helicopter configurations such as single main rotor/tail rotor, side by side rotors, tilting proprotor aircraft, and tandem rotor helicopters are available on CAMRAD. Flight conditions may vary from steady level flight, steady turns, to steady climb or descent conditions. A wind tunnel trim option is also available. Degrees of freedom are variable in the airframe, the rotor bending, and rotor torsion modes. The rotor wake may be modeled as uniform inflow or nonuniform inflow utilizing either a prescribed or free wake model. The standard helicopter disc orientation is shown in Figure 1A.

In rotorcraft dynamics, there are essentially two basic time scales. The rotor motion is periodic with a fundamental frequency of $\Omega/2\pi$, where Ω is the rotational speed. The airframe vibration is also harmonic with a frequency of $N\Omega/2\pi$, where N is the number of rotor blades. To solve the equations of motion, a harmonic analysis is first used to determine the periodic motion. The airframe motion can be assumed to be quasi-static compared to the rotor speed. Therefore, for the airframe trim calculations, the periodic rotor solution will be used for a more accurate representation of the helicopter motion and trim calculations.

CAMRAD begins with the trim analysis. The control positions and aircraft Euler orientation are determined for a specified operating condition. Assuming trim can be attained, the periodic blade motion is

then calculated, which leads to an evaluation of the rotor performance, loads, and noise. The trim solution can be attempted using uniform inflow, nonuniform inflow with a prescribed wake geometry, or nonuniform inflow with a free wake geometry, inflow being the airflow perpindicular to the rotor disc plane. Following the trim solution, the aeroelastic stability, flight dynamics, and transient analyses begin. The aeroelastic stability analysis determines the system stability. The aircraft flying qualities are determined from the rotor and airframe stability derivatives calculated in the flight dynamics analysis. The rigid body equations of motion are numerically integrated in the transient analysis for a prescribed control or gust input.

The section aerodynamic forces such as lift and drag are calculated using lifting line theory in conjunction with two dimensional airfoil characteristics, with corrections for three dimensional flow. First, the section velocity and pitch angles are evaluated, then the angle of attack and Mach number. The section aerodynamic coefficients are obtained by a linear interpolation of the two dimensional airfoil tables for a given angle of attack and Mach number. From the section aerodynamic coefficients, the section force components and moments are obtained. Then the section forces are integrated over the rotor radius to obtain generalized forces.

In order to examine the rotor structural behavior, an engineering beam model is used. A high aspect ratio of the structure (rotor) is assumed, making the beam theory applicable. The beam theory allows flap and lag bending with torsion of the rotor blade from large pitch and twist angles.

The first assumption of the engineering beam theory is that all plane sections perpendicular to the undeformed elastic axis of the blade remain so after bending of the blade. This assumption leads to a uniform strain over the section. The next assumption of the beam theory is that all stresses, except the axial stress, are negligible. This assumption simplifies the calculation of total moments due to bending and elastic torsion.

Essentially, in rotary wing analyses, there are four possible wake geometries. The rigid wake model, also known as uniform inflow, is the simplest. In the rigid wake model, the undisturbed helical geometry is utilized, in which all the wake elements are convected with the same mean velocity. This mean velocity is the air velocity seen by the blade section, consisting of helicopter forward speed, rotor and shaft motion, and wake induced velocity. If the flight condition is such that the wake is convected away from the rotor disk (large tip-path plane incidence at high speed, or high climb rates), obviously there will be no significant vortex-blade interaction, and this model will be satisfactory.

A slight improvement on the rigid wake model is the semirigid wake model. In this model, each wake element is convected downward with the induced velocity of the point on the rotor disk where it is created. The assumption that wake elements are convected with the velocity at the rotor disc is good for elements of small age ($\phi < 2\pi/N$), but not very accurate by the time the vortex is subject to the effect of the next blade. It can therefore be concluded that the semirigid wake model offers little

improvement over the rigid wake model. The semirigid wake model is not included on CAMRAD.

When the helicopter is operating such that the wake remains close to the rotor disc plane, there is much distortion from the basic helical geometry. Each wake element is convected with the local flow, which includes the velocity induced by the wake itself. This distorted wake geometry may be measured experimentally. A prescribed wake model utilizes this measured distortion, scaled to the appropriate operating conditions.

The free wake geometry is the most computationally complex of the wake models discussed. In the free wake model, the induced velocity is calculated at every element in the wake by summing the contributions from all elements in the wake. Then, these velocities are integrated to obtain the positions of the wake elements at the next time increment. The wake model for the free wake calculation consists of line segments for the tip vortices, and rectangular sheets for the inboard shed and trailed wake. The near wake or rolling up wake is not considered in the free wake model on CAMRAD. For the inboard vorticity in the free wake model, the prescribed wake geometry is still used. The distortion of the tip vortex from the basic helical shape is calculated in CAMRAD. Therefore, in order to reduce the complexity of the calculation procedure, the free wake model has been limited to the distortion of the tip vortex in calculating the induced velocity along the elements of the wake. Problems in the free wake model arise when vortex segments come into close contact with the

rotor blade. This gives rise to unduly large induced velocities and therefore wake displacements.

Occasionally, it is necessary to start the rotor instantaneously from rest, then continue the integration until a steady state geometry is obtained. A free wake analysis may be required to obtain a more accurate representation of the blade loading. For an operating condition that would give a small tip path plane incidence (such as low speed, moderate thrust, steady, level flight), the rigid wake model would predict that the tip vortices would always be convected downward. This downward convection places the tip vortices a considerable distance below the disc plane by the time the following blade encounters their place of origin. The free wake model, however, would predict that the tip vortices would still be in close vicinity of the disc plane, even when the next blade approaches. *The result is that the free wake model would more accurately show the blade loading to be considerably higher than that obtained from the rigid wake model.*

In CAMRAD, the aircraft control variables consist of collective and cyclic pitch of the two rotors and the aircraft flight controls. These controls consist of the engine throttle θ_t, wing flaperon angle δ_f, wing aileron angle δ_a, elevator angle δ_e, and the rudder angle δ_r. The transposed aircraft control vector can be expressed as:

$$\overline{v}^T = [\,(\theta_0\ \theta_{1c}\ \theta_{1s})_1\ (\theta_0\ \theta_{1c}\ \theta_{1s})_2\ \delta_f\ \delta_e\ \delta_a\ \delta_r\ \theta_t\,] \tag{1}$$

In the cockpit, the pilot's controls consist of collective stick δ_0 (positive upward), lateral cyclic stick δ_c (positive to the right), longitudinal cyclic stick δ_s (positive forward), pedal δ_p (positive for right yaw), and the throttle δ_t. The transposed pilot control vector is given as:

$$\overline{v}_p{}^T = [\ \delta_0\ \ \delta_c\ \ \delta_s\ \ \delta_p\ \delta_t] \tag{2}$$

In the CAMRAD trim solution, a linear relationship between the pilot's control inputs and the rotor and aircraft control variables is utilized. The aircraft control vector is defined as:

$$\overline{v} = T_{CFE}\, \overline{v}_p + \overline{v}_0 \tag{3}$$

$\overline{v}_0$ is the control input with all sticks and the pedal centered or $\overline{v}_p = 0$. T_{CFE} is a transformation matrix which is defined by the control system geometry. The transformation matrix is governed by control gains (rotor degrees per degree of stick deflection) and swashplate azimuth lead angles (degrees). Reference 1 shows the exact contents of T_{CFE} for various helicopter airframe configurations.

From closer analysis of T_{CFE} it can be seen that the collective pitch of

both rotors is governed by collective and longitudinal cyclic stick

displacement. The lateral cyclic pitch is defined by lateral cyclic stick

and pedal displacement. If the swashplate azimuth lead angles were non-

zero, the longitudinal cyclic pitch would be defined by lateral cyclic stick

and pedal displacement. For the BV360, all azimuth lead angles are zero.

Because T_{CFE} uses the sine of the swashplate azimuth lead angles to

determine the longitudinal cyclic pitch, it is obvious that the rotor

longitudinal cyclic pitch only depends upon the stick centered values of

longitudinal cyclic pitch. The stick centered values also affect the rotor

collective and lateral cyclic pitch as shown before.

Figure 1 shows the collective pitch measurement with blade angle

correlation as measured in the Boeing Vertol Whirl Tower test of the

Model 360, and presented in Reference 2. The 1:1 correlation curve

illustrates the theoretical actuator to blade angle correlation given zero

blade twist, stick gain, swashplate azimuth lead angle, and control

deviation. The faired curve, however, shows the actual blade angle

correlation at a rotor speed of 270 RPM. The twist and gain differences

between the actuator and the 0.75 radial station is evidenced by the blade

angle offset of -5.25 degrees at the collective actuator setting of 0

degrees. The nonlinearity of the actual blade angle correlation at the

higher collective actuator settings indicates the presence of control "slop"

in the BV360. At present, CAMRAD does not account for this control

deviation. Its presence indicates that CAMRAD's control value prediction

must be corrected at the higher actuator angle values for an accurate

comparison to the actual BV360.

For axial flight, the rotor is said to be in the normal working state when climbing or hovering. In this state, the vertical velocity, V, and the induced velocity, v, are both flowing downward through the rotor disc. In descent conditions, three possible flow states may exist at the rotor. In partial power descents, the upward component of the freestream velocity keeps the blade tip vortex spirals piled up under the disc, forming the vortex ring state. Eventually, the strength of the ring vortex is great enough to cause its separation from the disc plane. This separation causes an unsteady breakdown of the flow. In autorotation, the turbulent wake state is created. Ideally, there is no flow through the disc, but recirculation leads to a considerable amount of flow turbulence in the turbulent wake state. The windmill brake state is formed at large rates of descent ($V<-2v_h$). In this state, a definite slipstream is once again established because of a well behaved wake above the rotor.

In estimating the induced and profile power, momentum theory gives a good estimate in hover if an empirical factor is included to account for additional induced losses such as tip losses and those due to nonuniform inflow. It is in question whether momentum theory can accurately predict the power requirements for descent conditions.

The energy required to produce helicopter thrust is known as induced power, P_i. To overcome rotor drag and turn the rotor, profile power, P_o, is necessary. The induced power is given as $P_i= Tv$, where v is the induced

velocity at the rotor disc. The induced velocity is a function of speed, thrust, rotor disc area, air density, and disc angle of attack.

$$v=f(V,T,A, \rho, \alpha) \tag{4}$$

From momentum theory, the hover induced velocity is defined as

$$v_h=(T/2\rho A)^{1/2}. \tag{5}$$

The parameter v/v_h is equivalent to P_i/P_h, which is the ratio of induced power to momentum theory hover power.

The momentum theory can be utilized to give the following results for the rotor in climb:

$$v= -V/2+ [(V/2)^2+(v_h)^2]^{1/2} \tag{6}$$

For the rotor in descent, the induced velocity is given as

$$v= -V/2- [(V/2)^2-(v_h)^2]^{1/2} \tag{7}$$

with V being the vertical velocity. Using these results the rotor induced power in vertical flight can be determined as shown in Figure 2. Available experimental data from Washizu, Azuma, Kou, and Oka is also plotted on

Figure 2, and is available in Reference 3. In both the normal working and windmill brake states, Figure 2 shows good correlation to momentum theory. For hover and climb conditions, the experimentally measured induced power is higher than the momentum theory results by a small, nearly constant factor. This discrepancy can be accounted for due to additional losses of a real rotor from tip losses, nonuniform inflow, tip Mach number, and blade twist. In the vortex ring state, the correlation to momentum theory differs considerably. Because of the highly turbulent and unsteady flow characteristics of the vortex ring state, a uniform inflow assumption such as momentum theory cannot accurately predict the performance parameters associated with this condition.

III. Boeing Vertol Helicopter Model 360

The Boeing Vertol Model 360 is known as a "soft rotor system." The blades of the BV360 are less restricted in their movements in the flap direction, lag direction, and torsional plane than conventional rotor designs. The BV360 is an articulated rotor, consisting of lead-lag, feathering, and offset hinges. The hinged rotor design also allows for more blade movement than a hingeless or teetering rotor. The BV360 rotor uses the advanced VR12 and VR15 airfoil sections. Also present in the BV360 rotor system is a 3:1 taper ratio in the tip region and virtually all composite blades. The highly tapered tip region helps alleviate the tip

loss of the rotor. Because actual blade loading drops to zero at the tip, a smaller effective area is present in the wake, thus increasing the induced power loss. The BV360's taper ratio allows the actual blade loading to conform closer to that predicted by lifting line theory. This increase in effective disc area combined with the clean drag design of the BV360 yields a 200+ knot rotor system, as described in Reference 4. The BV360 blade planform is shown in Figures 3 and 4, and was obtained from Reference 5.

In helicopter analysis, torsional stiffness is the resistance to torque about the radial axes of the blade. Figure 5 shows the radial distribution of torsional stiffness of·the BV360. For the untapered blade section, the torsional stiffness is constant, with a fairly high resistance to torque. In the tip region, however, the torsional stiffness rapidly declines, indicative of increased blade twisting in the tip region. Comparisons can be made to conventional technology rotors such as the CH-46 and OH-6. As seen in Figure 6, these rotors exhibit a uniform distribution of torsional stiffness from root to tip. The CH-46 and OH-6 are obviously much stabler blades about the radial axis.

The flapwise bending stiffness indicates a system's resistance to forces in the z-plane. Figure 7 shows the BV360 with minimal flapwise bending stiffness outside the hub region. Figure 8 shows the conventional rotors displaying a much greater resistance to flapping motion due to blade loading and perturbations.

The chordwise bending stiffness determines the rotor's response to

forces in the x-plane. Referring to Figure 9, the BV360 possesses approximately uniform radial distribution of chordwise bending stiffness. In the tip region, the stiffness decreases significantly. Figure 10 indicates that the conventional rotors are also much stiffer in the chordwise bending plane, with a uniform stiffness distribution from root to tip.

In a tandem rotor helicopter, the height control, or vertical force, is controlled by the main rotor collective. Directional or yaw control is achieved using main rotor differential cyclic. Lateral or roll control is governed by the main rotor cyclic. Longitudinal control of the pitch moment is achieved using main rotor differential collective. Therefore, to reach the trim condition on a tandem rotor helicopter, collective, differential collective, lateral cyclic, and differential lateral cyclic are utilized. It is important to note that longitudinal cyclic control is not included in the controls necessary to realize the trim condition. Collective pitch, lateral cyclic pitch, and longitudinal cyclic pitch all have initial values of displacement with the pilot's controls centered. After reaching trim, the longitudinal cyclic pitch of both rotors remains at this "stick centered" displacement. Although this seems to be a limiting factor on the ability of the aircraft to reach trim, actually, the differential collective assumes the role of the longitudinal cyclic control on the tandem rotor helicopter.

IV. EXPERIMENTAL DESCRIPTION

In July, 1986, a pressure gage instrumented model rotor was tested by the Boeing Vertol Company and the Army Aeroflightdynamics Directorate (AFDD), with NASA Ames participation, in the Duits-Nederslandse Windtunnel (DNW), as described by Reference 6. Using the results from this testing, a comprehensive study has been undertaken to determine if the test conditions investigated in the DNW can be accurately recreated in actual free flight testing with the Boeing Vertol Model 360. It will be necessary to eventually fly the full scale prototype aircraft at these conditions simulated in the DNW. In order to ensure the most efficient use of this flight test time, CAMRAD was investigated to determine its usefulness in creating the prototype's flight test matrix. Confidence in CAMRAD comes through its wind tunnel comparisons with the DNW results. Then prototype trimmed flight test controls are predicted. Finally, the full scale BV360 will be flown at these settings.

The wind tunnel analysis was conducted with the front rotor alone, without the rear rotor or fuselage. CAMRAD was run to trim the rotor on C_T/σ and XBAR using collective, lateral cyclic, and longitudinal cyclic pitch. CAMRAD was run using uniform inflow, a prescribed wake model, and a free wake model. Also varied were the degrees of freedom allowed in the rotor vibratory solution.

Although the model used in the DNW testing was a 1:5 scale model of the actual BV360, control settings such as collective, lateral cyclic, and longitudinal cyclic are parameters which are not affected by size

scaling. Also investigated were the shaft angle, thrust coefficient, and the advance ratio. Both μ and C_T/σ are nondimensionalized by the tip speed of the rotor blade, therefore implicitly scaled.

The data from the DNW testing of the model BV360 was reevaluated in December, 1987. Much was done to ensure that each recreation on CAMRAD of a DNW test point closely resembled the actual test condition. The sound speed (a) measured in the DNW was used to determine a standard day temperature for CAMRAD by:

$$TEMP\ (\ R)=a^2/\gamma R \tag{8}$$

The DNW air density was also input to CAMRAD. CAMRAD was also provided with rotor RPM, forward speed, and helicopter weight as determined from DNW values of M_{tip}, μ, and C_T/σ.

$$RPM= M_{tip}{}^*a^*60/R/2\pi \tag{9}$$

$$Forward\ speed= \mu^*V_{tip} \tag{10}$$

$$Weight=C_T/\sigma^*\sigma^*\rho^*(V_{tip})^{2*}(disc\ area) \tag{11}$$

Unless otherwise specified, the shaft angle of attack, longitudinal tip path tilt angle, β_{1c}, and the lateral tip path tilt angle, β_{1s}, will remain unchanged in the trimmed solution. For the shaft angle, this is not an overly unusual condition. A trimmed shaft angle of $0^\cdot$ indicates the shaft

is perpendicular to the free stream. Trimmed values of β_{1c} and β_{1s} equal to $0^{\cdot}$ in forward flight are virtually impossible. This condition indicates that there is no flapping of the rotor blades longitudinally or laterally. In light of the extraordinary softness of the BV360 blade, flapping will definitely occur in any operating condition except hover, perhaps. When β_{1s} and β_{1c} were not given values on which to trim, in many instances the rotor thrust coefficient was found to be negative, or at a much lower value than, the rotor lift coefficient. The lift coefficient, perpendicular to the free stream, can be defined as $C_L = C_T \cos\alpha + C_H \sin\alpha$, where C_H is the rotor drag coefficient, and α is the angle between the shaft axes and the freestream. To obtain a negative thrust coefficient with a positive drag coefficient, it would be necessary for the aircraft to be inclined past $\alpha = 90^{\cdot}$, or practically be inverted.

V. Results

A. Comparison of CAMRAD to DNW Tests

All of the DNW test conditions analyzed were in the open jet configuration. The first test condition was an advance ratio sweep at

C_T/σ =0.07, hover tip Mach number of 0.636, and XBAR=0.05. The advance

ratio in this test condition varied from 0.15 to 0.36. CAMRAD was utilized

to simulate a wind tunnel test configuration with uniform inflow at the

isolated rotor. The merit of the various parameters investigated in

CAMRAD largely depends on the proximity of the trimmed control variables

to the input DNW values. In this test condition, the above mentioned

performance parameters are the control variables, whereas the rotor

collective, lateral cyclic, and longitudinal cyclic are the variables under

investigation.

For all test points modeled on CAMRAD, the hover tip mach number was

input as a constant, and did not vary with the trim solution. The values of

C_T/σ and XBAR were also input from the trimmed DNW values. The wind

tunnel trim option used in this analysis attempted to trim the rotor on

given C_T/σ and C_X/σ values by varying the rotor controls of collective,

lateral cyclic, and longitudinal cyclic. Because CAMRAD attempts to reach

the trim condition from the operator inputs, it is necessary to carefully

determine the initial pilot control variables. Referring to Figure 11, it can

be seen that the trimmed solutions from CAMRAD compare very well to the

input DNW values of C_T/σ. The average trimmed value of C_T/σ from the

CAMRAD solution is 0.07119. The DNW average C_T/σ was 0.0698, a

difference of only 1.99%. It was observed that at lower advance ratios,

CAMRAD did not trim to the thrust coefficient as closely as at higher

advance ratios. Figure 12 shows the variation of rotor thrust coefficient with shaft angle. At higher values of shaft angle (low advance ratios) again it is seen that CAMRAD did not trim as well to the DNW values of thrust coefficient as at the lower values of shaft angle. Figure 13 shows the variation of the rotor propulsive coefficient with advance ratio. The CAMRAD test points show very good correlation with the trimmed DNW propulsive coefficient values. In regards to trimming the propulsive force, CAMRAD now exhibits better correlation at the lower advance ratios to the DNW conditions. Figure 14 reemphasizes this finding by showing better correlation to propulsive coefficient at the higher values of shaft angle. The average value at this test condition of XBAR, the nondimensionalized propulsive force in the wind coordinate system, was 0.05 in the DNW. CAMRAD gave an average trimmed value of 0.0448 for XBAR, differing by 10.4%. This deviation is attributable to the poor correlation at the highest advance ratio. Excluding the trimmed value of XBAR from CAMRAD at the advance ratio of 0.355, the CAMRAD XBAR values differ from the DNW by only 3.47%. The control variables modelled on CAMRAD compare well to the actual values taken at the DNW.

To check the validity of CAMRAD on reproducing the actual rotor control angles needed to achieve trim in a given flight condition, the control angles from the wind tunnel analysis were investigated. After reaching trim, CAMRAD gives the pilot's controls necessary to reach the trim condition. These values were then transformed to the actual blade actuator settings as described in Part II, and corrected for the -3.55

degrees of twist from the blade root to the 75% radial station. The control "slop" as described in Part II was not used in the analysis due to its nonlinearity with collective settings. Figure 15 shows the variation of collective pitch at the 75% radial station with advance ratio at this given test condition. At an advance ratio above 0.3, the DNW results show that the collective pitch increases rapidly to meet the requirement of a dramatic increase in the forward thrust component. Also from Figure 15, it can be seen that CAMRAD predicts collective pitch angles very similar to those from the DNW in the intermediate advance ratio range of 0.2 to 0.3. The most deviation in a CAMRAD trimmed solution occurs at the advance ratio of 0.355, with a collective pitch difference of 1.07 degrees. At an advance ratio of 0.15, the collective pitch differs by 0.8 degrees. This is an acceptable amount of deviation at these advance ratios. Referring to Figure 16, it can be seen that CAMRAD exhibits excellent correlation of lateral cyclic pitch to the DNW results. Because of the wind tunnel analysis, lateral control of the roll moment is easily trimmed by CAMRAD. Figure 17 shows that again, CAMRAD exhibits excellent correlation to the DNW results, now, in reference to the longitudinal cyclic pitch. In regards to longitudinal control, it is obvious that that values of longitudinal cyclic pitch do vary with different operating conditions. Analogous to a single main rotor and tail rotor helicopter, the model tandem rotor, as only a single rotor, must use longitudinal cyclic to trim the pitching moment when it does not have use of differential collective. The slight deviation from the DNW results can be attributed to the

difficulty in trimming the propulsive coefficient and the thrust coefficient, which both contain components in the longitudinal axis.

The discrepancy at advance ratios below 0.2 may be explained by the inaccuracy of the wake model. A simple computer program was written to plot the rigid wake as determined by the rotor advance ratio as it unrolls from an input reference blade. Referring to Figures 18 and 19, it can be seen that at the advancing blade position, the trailed vortices from the four blades all cross the reference blade at least one time in a four revolution time period. The trailed vortex of the blade at $\psi=0°$ crosses the reference blade twice. The possibility of five blade vortex interactions on any given blade at a low advance ratio is not included in the uniform wake model on CAMRAD. Because these interactions would significantly alter the blade loading, it may be said that the uniform wake model may not give an accurate representation of the required control positions at low advance ratios.

There are two possible explanations for the control discrepancies at the higher advance ratios ($\mu>0.30$). First, in the actual wind tunnel, it can be shown that the blade wake is convected away from the rotor disc quickly at high advance ratios. This wake convection is not accurately modelled by the uniform wake model on CAMRAD. The effects of compressibility may also explain the control discrepancies. At an advance rato of 0.35, the advancing tip Mach number is in excess of 0.8 outboard of the 90% radial station. The BV360 has a specially designed tip section to allow for high speed operation while delaying the effects of Mach drag

divergence. CAMRAD utilizes two dimensional airfoil data with tip relief corrections. These corrections may give a lower blade lift distribution than is actually present. Because of this lift deficiency, the system may therefore increase blade collective pitch.

The next set of test conditions investigated was a descent array with a shaft angle sweep at various advance ratios and values of propulsive coefficient. The control variables were the hover tip Mach number of 0.636, and $C_T/\sigma = 0.069$. All of these test points were modelled with a positive shaft angle (aft tilt) and a negative propulsive coefficient (in the drag direction).

CAMRAD was run with a uniform wake, prescribed wake, and free wake model for all of the descent conditions. A negative value of C_X/σ was never obtained when CAMRAD was allowed to trim only on the input value of C_T/σ. Although CAMRAD did reach a state of trim, this discrepancy in the trimmed value of propulsive coefficient combined with the large variation in actual rotor control settings does not allow for any correlation to be drawn to the DNW results. When modelling CAMRAD to trim on the input value of C_X/σ, the trim condition was never realized, regardless of the wake model utilized. Because of the possible presence of the vortex ring state in the rotor wake in a partial power descent, the flow unsteadiness necessary to achieve a negative value of C_X/σ may not be accurately reproduced on any of CAMRAD's momentum theory wake

models.

From the wind tunnel analysis, it can be concluded that CAMRAD can be accurately used to simulate forward flight wind tunnel test conditions. At the present time, the method necessary to allow CAMRAD to predict partial power descent in the wind tunnel is unknown.

B. Prediction of Trim Conditions

CAMRAD has been determined to be an accurate analytical model in reproducing wind tunnel simulation of forward flight for the Boeing Vertol Helicopter Model 360. Its validity in reproducing forward free flight will be discussed next.

In the free flight option of CAMRAD, the helicopter is attempting to reach the trim condition by trimming all forces and moments to zero through use of the collective pitch, lateral and longitudinal cyclic pitches, pedal displacement (not utilized in the isolated rotor wind tunnel option), aircraft pitch, and aircraft roll angles. From initial analysis of the full scale BV360 in free flight, the trimmed control positions always indicated that the longitudinal cyclic pitch of both rotors remained unchanged, regardless of the operating condition. As discussed earlier, this is characteristic of a tandem rotor.

Before CAMRAD can be used to construct a matrix of rotor control settings for various operating conditions, it must be ensured that the free flight simulation is accurate. The forward flight conditions from the DNW

were used to determine CAMRAD's free flight validity. From Figure 20, it can be seen that CAMRAD does reproduce comparable values of thrust coefficient in the free flight configuration. Figure 21 compares the DNW values of propulsive coefficient to those obtained from CAMRAD. A significant difference between values is noted. This may be explained by the fact that the propulsive coefficient is dictated by the drag on the system. In the wind tunnel, the only drag forces present are those from the single rotor. In the free flight configuration, however, drag is also present from the second rotor, the fuselage, and any rotor-rotor interference effects. What is important to note in Figure 21 is the similar slopes between the free flight and wind tunnel curves. The slope similarity gives confidence in CAMRAD's prediction of required propulsive force. Figures 22 through 25 compare the azimuthal lift distribution for various flight conditions of free flight and wind tunnel configurations. Actual lift distributions from the DNW testing is not yet available. Therefore, the lift distributions from the already validated CAMRAD wind tunnel analyses were used. Again, a direct correlation can not be made from the free flight to the wind tunnel results because of the difference in configurations. From these figures however, the phase of the peaks and troughs of the azimuthal lift distribution in free flight can be said to be comparable to that obtained in the wind tunnel. Although the magnitude of the free flight lift distribution predicted by CAMRAD does differ significantly from the wind tunnel analysis, without actual lift data, no conclusions can be made on this discrepancy. Also important is the fact

that both the wind tunnel and free flight CAMRAD analyses show the azimuthal lift distribution as a one per revolution periodic occurrence. This correlates well to theory presented in Reference 7. It can be communitatively concluded that CAMRAD is a valid tool for predicting free flight of the BV360.

All free flight conditions analyzed on CAMRAD were with the uniform wake model. Nonuniform inflow with a prescribed wake model and a free wake model were attempted for free flight. CAMRAD did not obtain motion or circulation convergence using nonuniform inflow with the BV360. It is important to note that the conventional technology CH-46 and OH-6 rotors did achieve trim with the prescribed wake model. The significant differences between the conventional rotors and the BV360 are the aeroelastic characteristics. It may be that the "softer" rotor.may require smaller time increments in the azimuthal stepping to achieve convergence. For a "soft" rotor, a 10 degree azimuth step may not accurately predict the actual blade motion. Steps of 3 to 5 degrees may be required.

In the free flight configuration, CAMRAD was used to construct a matrix of control settings necessary to realize various advance ratios at given thrust coefficients. CAMRAD was run at advance ratios of 0.17, 0.23, and 0.29, with gross weights of 27500, 29000, and 30500 pounds. These weights correspond to values of C_T/σ of 0.06312, 0.06656, and 0.0700, respectively. Figure 26 shows a linear variation of thrust coefficient with advance ratio for a given gross weight. This is the expected result for a fixed rotor rotational speed. Figure 27 shows the

collective pitch angle at 75% radius at these points. Figure 28 shows the variation of lateral cyclic pitch at these operating conditions. Figure 26 can be used by the designer to determine the gross weight required for a given advance ratio and rotor thrust coefficient. Figure 27 and 28 will then give the necessary collective pitch and cyclic control for trimmed flight. At the present time, this free flight control matrix has not yet been tested, but is expected to be utilized in future tests of the BV360 helicopter.

VI. Concluding Remarks

CAMRAD, at present, does not have the ability to predict the pressure distribution on the rotor blades. The pressure distribution would allow the code to be further validated in many areas because of the fundamental nature of this distribution in all testing. The smallest azimuthal variation available on CAMRAD is 10 degrees. Although this is a suitable increment for average power and load distributions, for any acoustic blade vortex interaction study, CAMRAD will require a more exacting increment. A smaller azimuthal increment may also be necessary to examine nonuniform inflow free flight on the BV360. CAMRAD has been determined to be a suitable analytical model for determining a forward free flight test matrix for the prototype Boeing Vertol Helicopter Model 360. The CAMRAD wind tunnel analysis compared well to the DNW results in all areas investigated of the forward flight cases. The small discrepancies noted

may be caused by the inefficiency of CAMRAD in its low speed wake model and its modelling of compressibility effects. These discrepancies may also be due to inaccuracies in data acquistion and reduction. The free flight simulation on CAMRAD produced results that correlate well to basic helicopter aerodynamic theory.

VII. References

1. Johnson, Wayne: A Comprehensive Analytical Model of Rotorcraft Aerodynamics and Dynamics Part 1: Analysis Development. NASA TM 81182, 1980.

2. Mills, S.: Model 360 Rotor Whirl Test Aerodynamic Performance Evaluation. Boeing Vertol IOM 8-7442-1-1015, July, 1987.

3. Johnson, Wayne: Helicopter Theory. Princeton University Press, Princeton, New Jersey, 1980.

4. Watts, M.E.; and Cross, J.L.: The NASA Modern Technology Rotors Program. AIAA Paper 86-9788, 1986.

5. Wiesner, R.: Model 360 Data for Rotor Performance Predictions. Boeing
    Vertol IOM 8-7050-2-228, December, 1985.

6. Dadone, L.; Dawson S.; and Ekquist, D.: Model 360 Rotor Test at DNW-
    Review of Performance and Blade Airload Data. American Helicopter
    Society Annual Forum, St. Louis, Missouri, May 1987.

7. Prouty, R.W.: Helicopter Performance, Stability and Control. PWS
    Publishers, Boston, Massachusetts, 1986.

FIGURE 1A: Rotor Orientation System
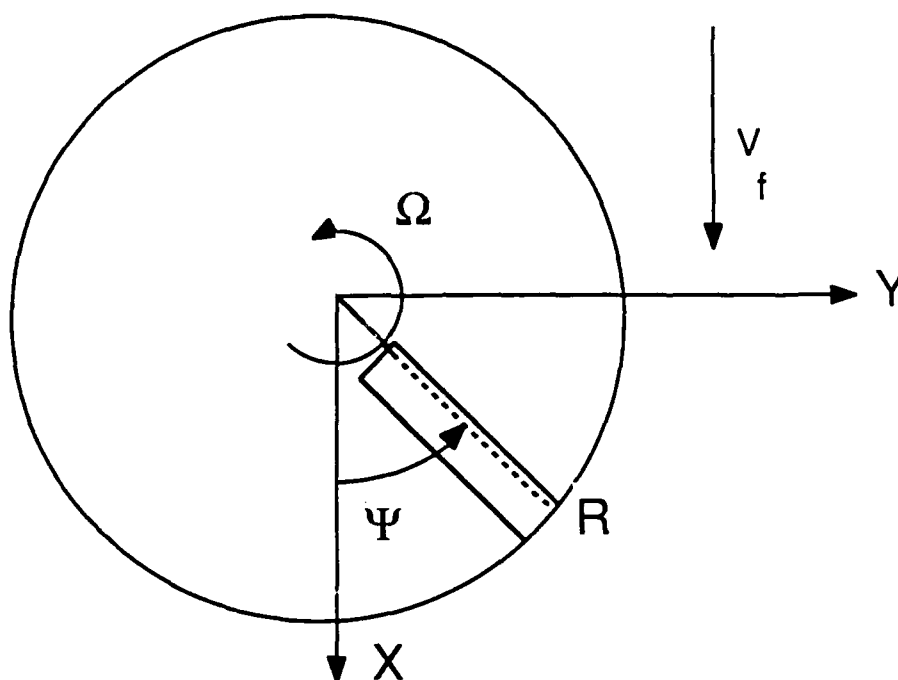
FIGURE 1: Collective Pitch Measurement
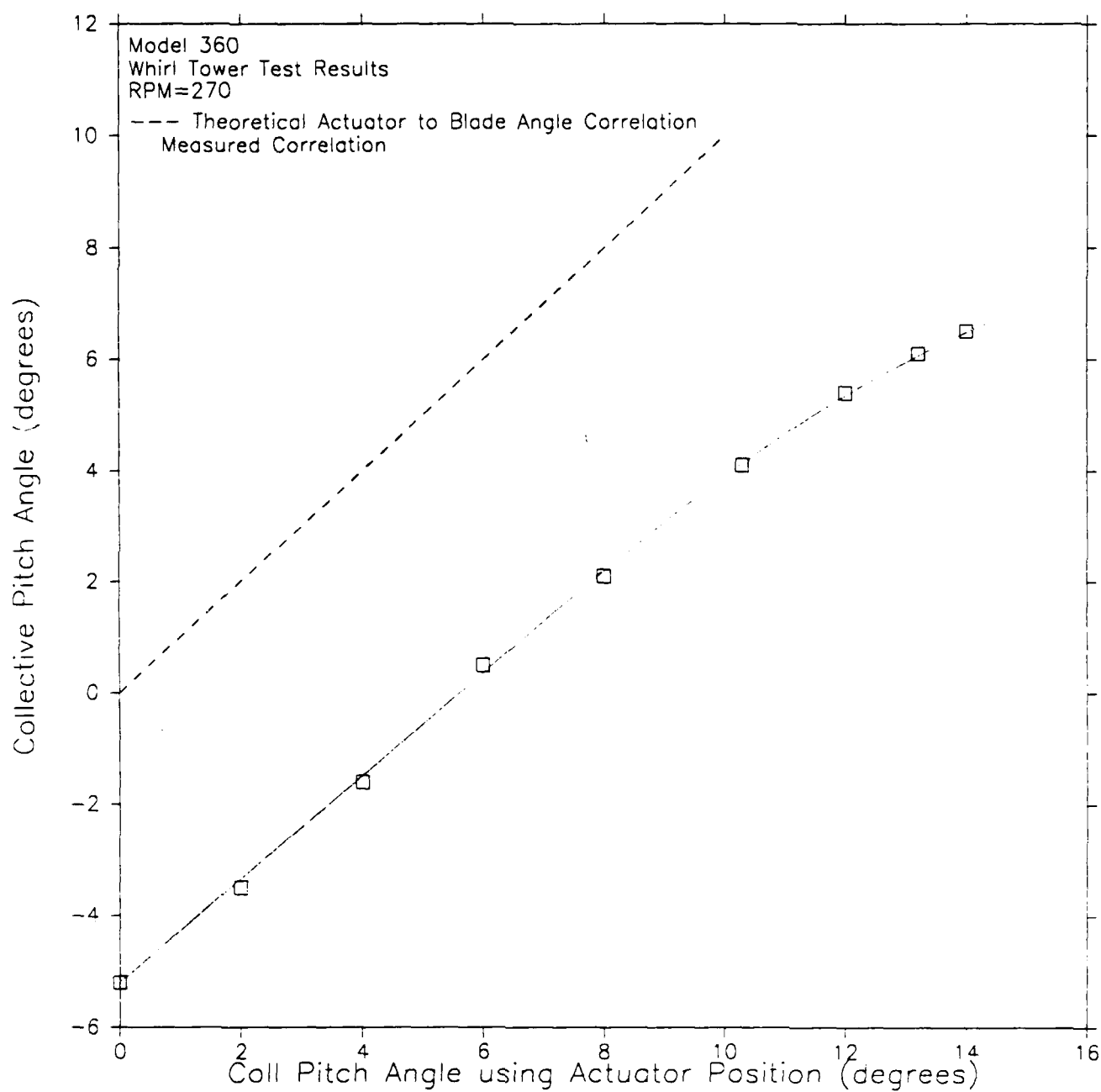
FIGURE 2: Induced Velocity in Forward Flight
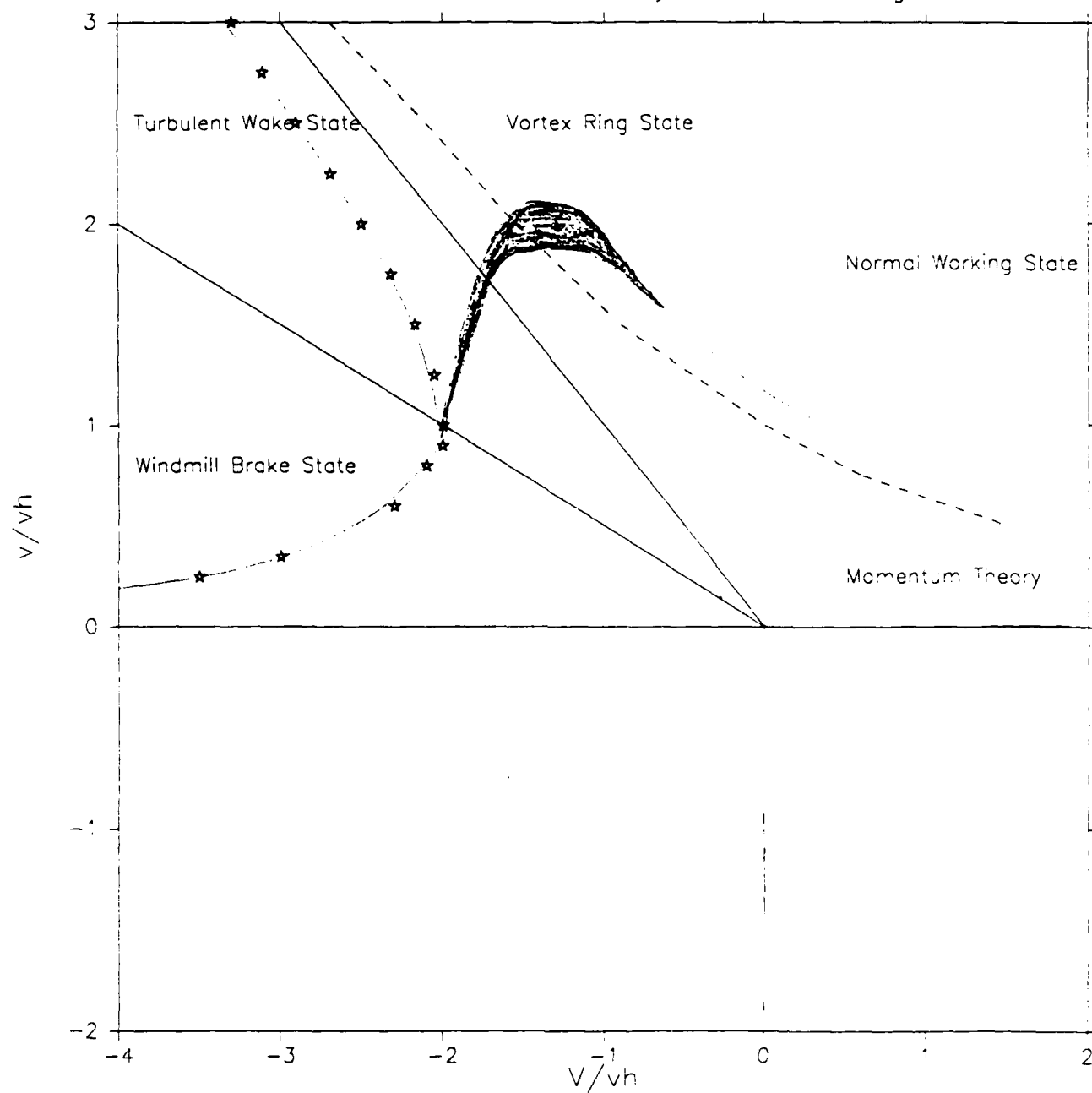
FIGURE 3: Boeing Vertol Model 360 Blade Planform

VR12 Airfoil from 0.25< r/R <0.88
VR15 Airfoil from 0.88< r/R <1.0
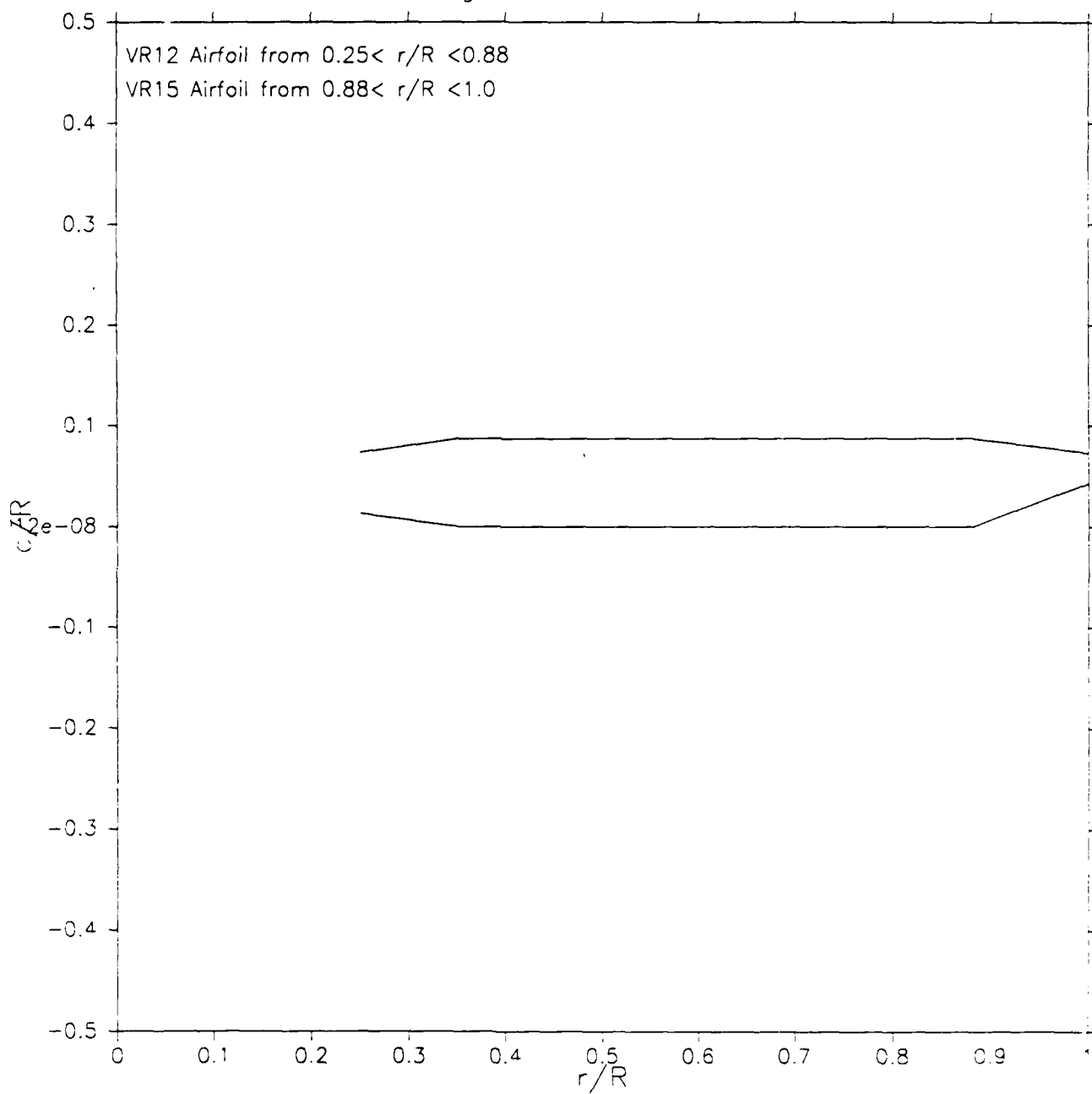
FIGURE 4: Boeing Vertol Model 360 Blade Planform
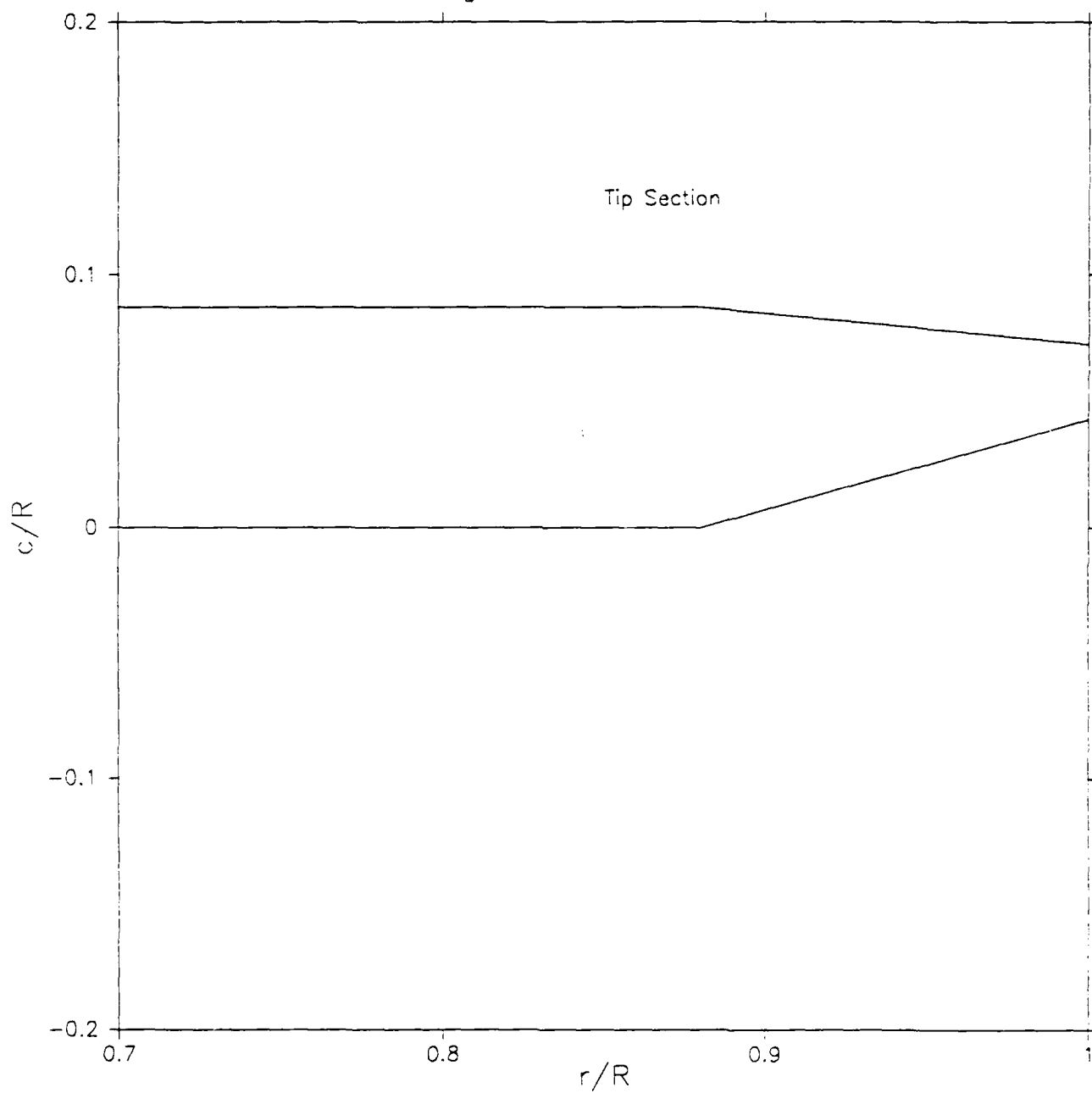
FIG 5: Normalized Torsion Stiffness vs Radius of BV360
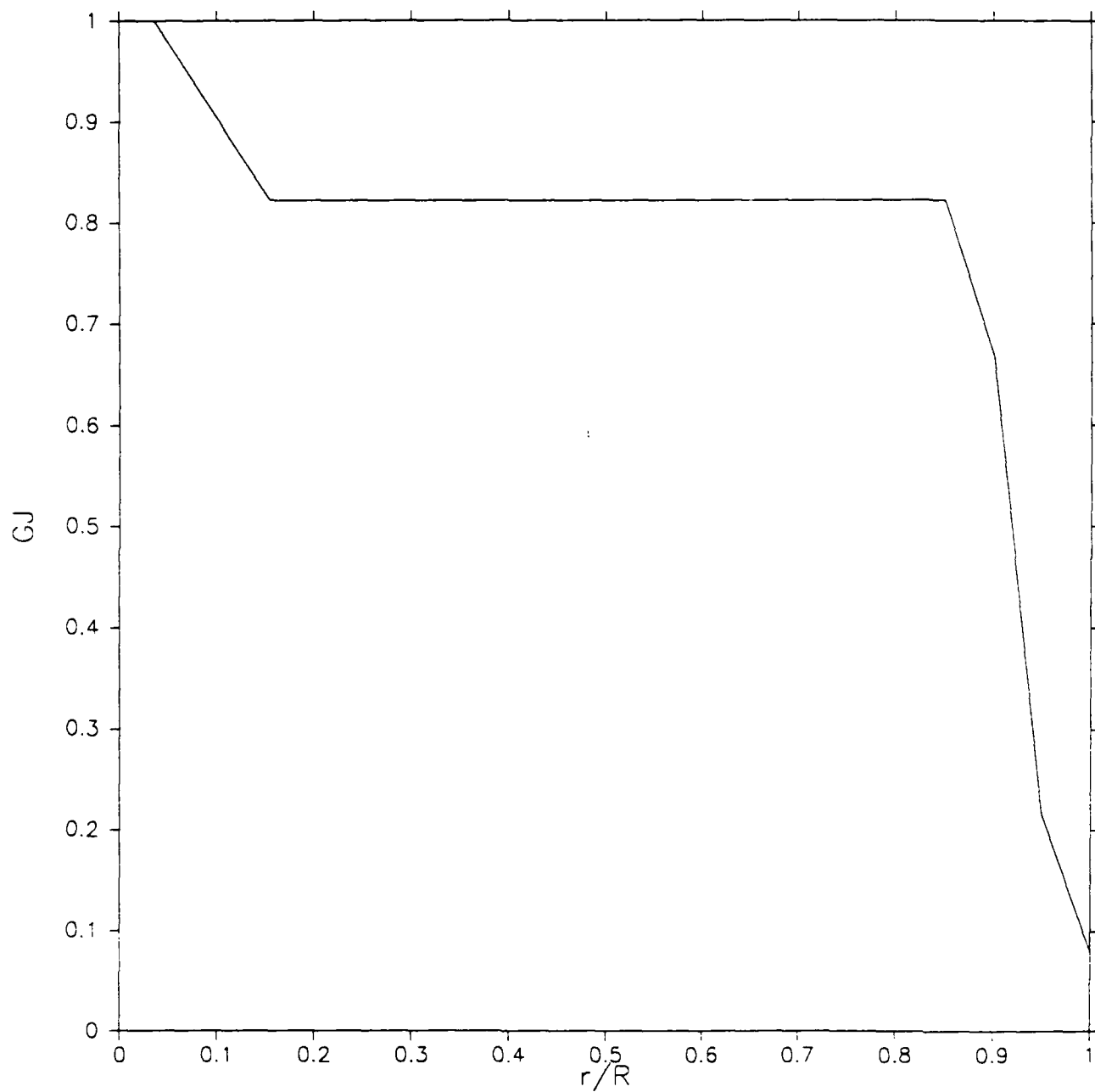
FIGURE 6: Normalized Torsional Stiffness vs Radius
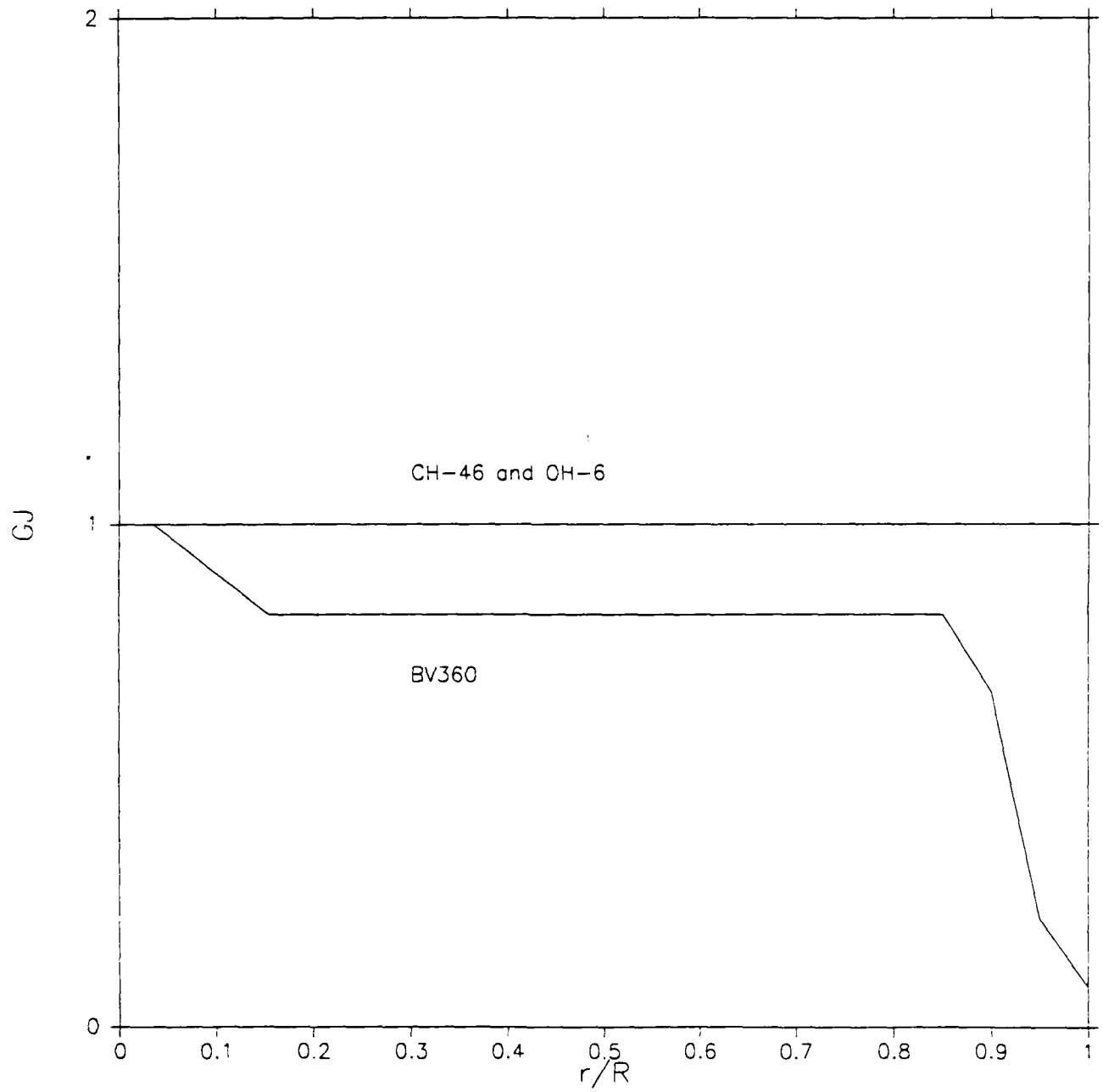
FIG 7: Normalized Flap Bending Stiff vs Radius of BV360
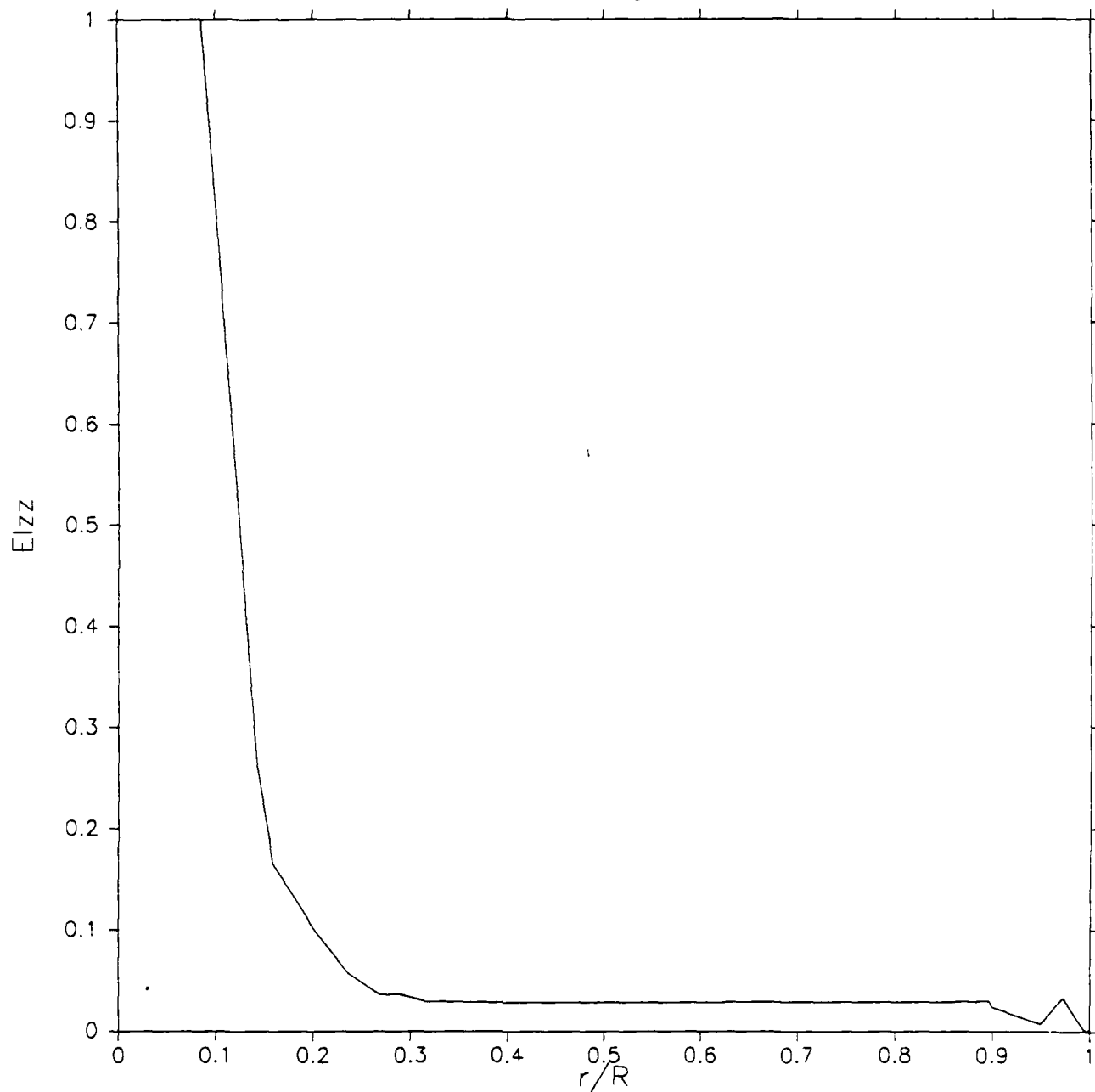
FIG 8: Normalized Flap Bending Stiff vs Radius
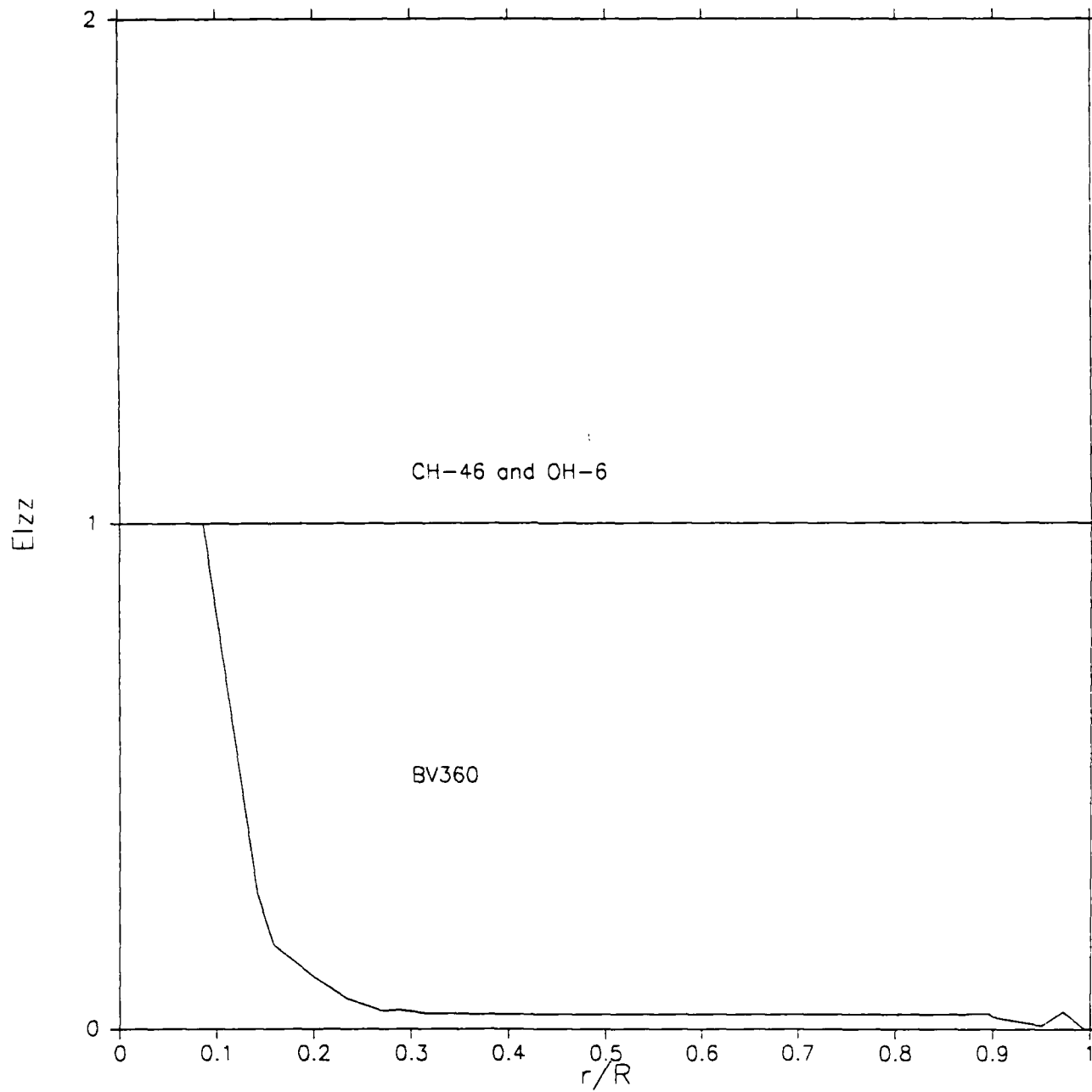
FIG 9: Normalized Chordwise Bending Stiffness of BV360
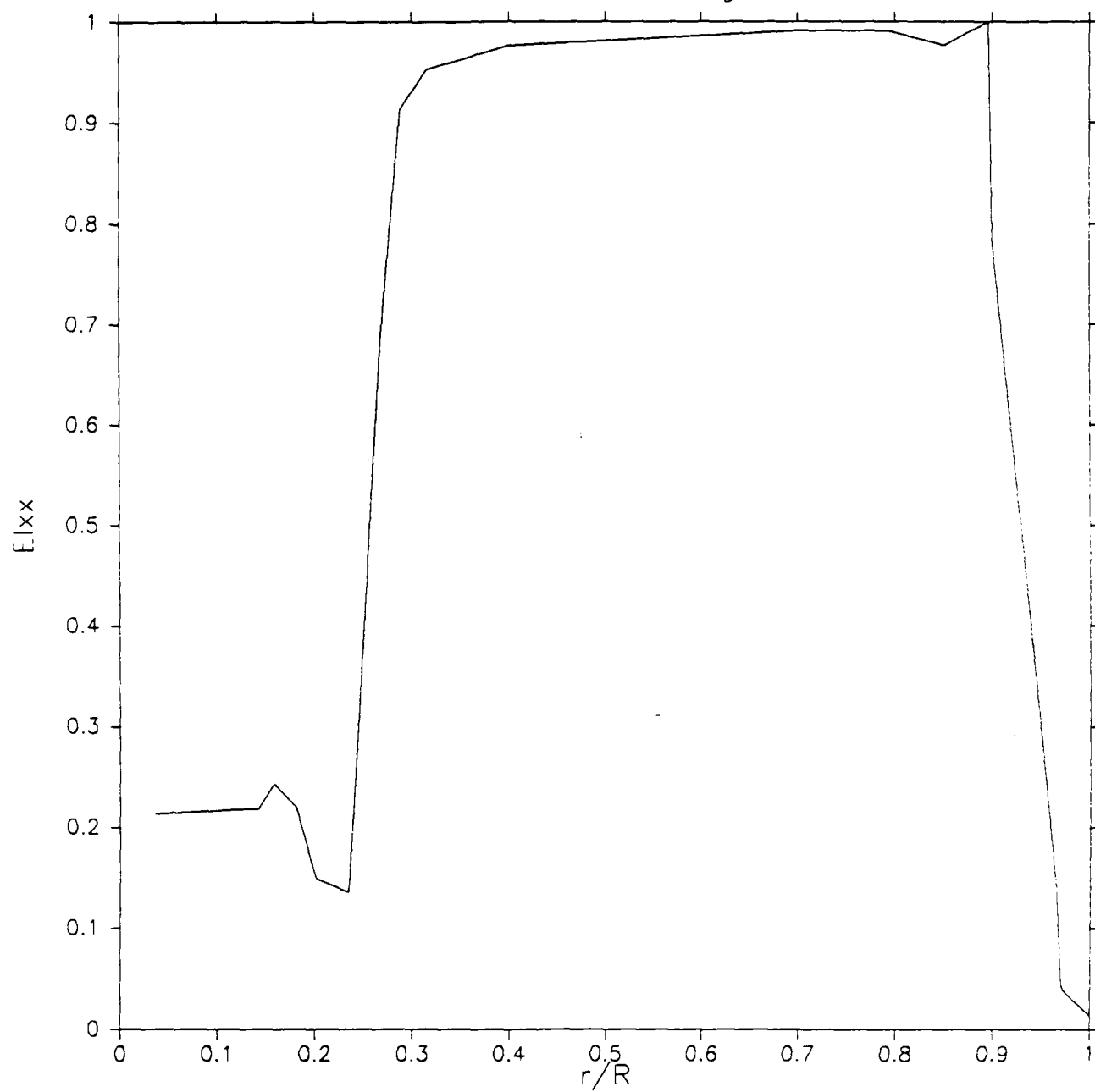
FIG 10: Normalized Chordwise Bending Stiffness
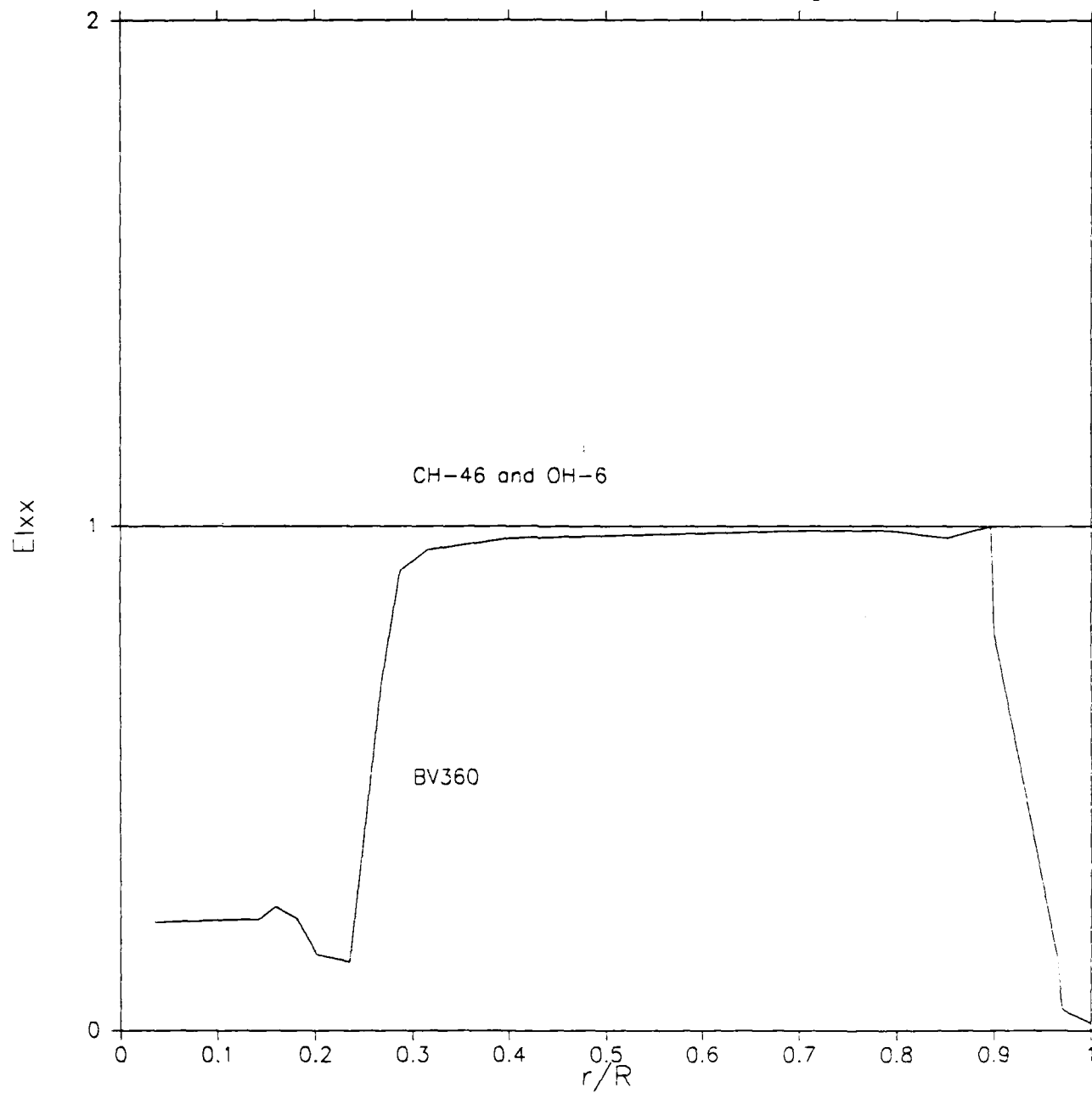
FIGURE 11: Thrust Coefficient vs Advance Ratio
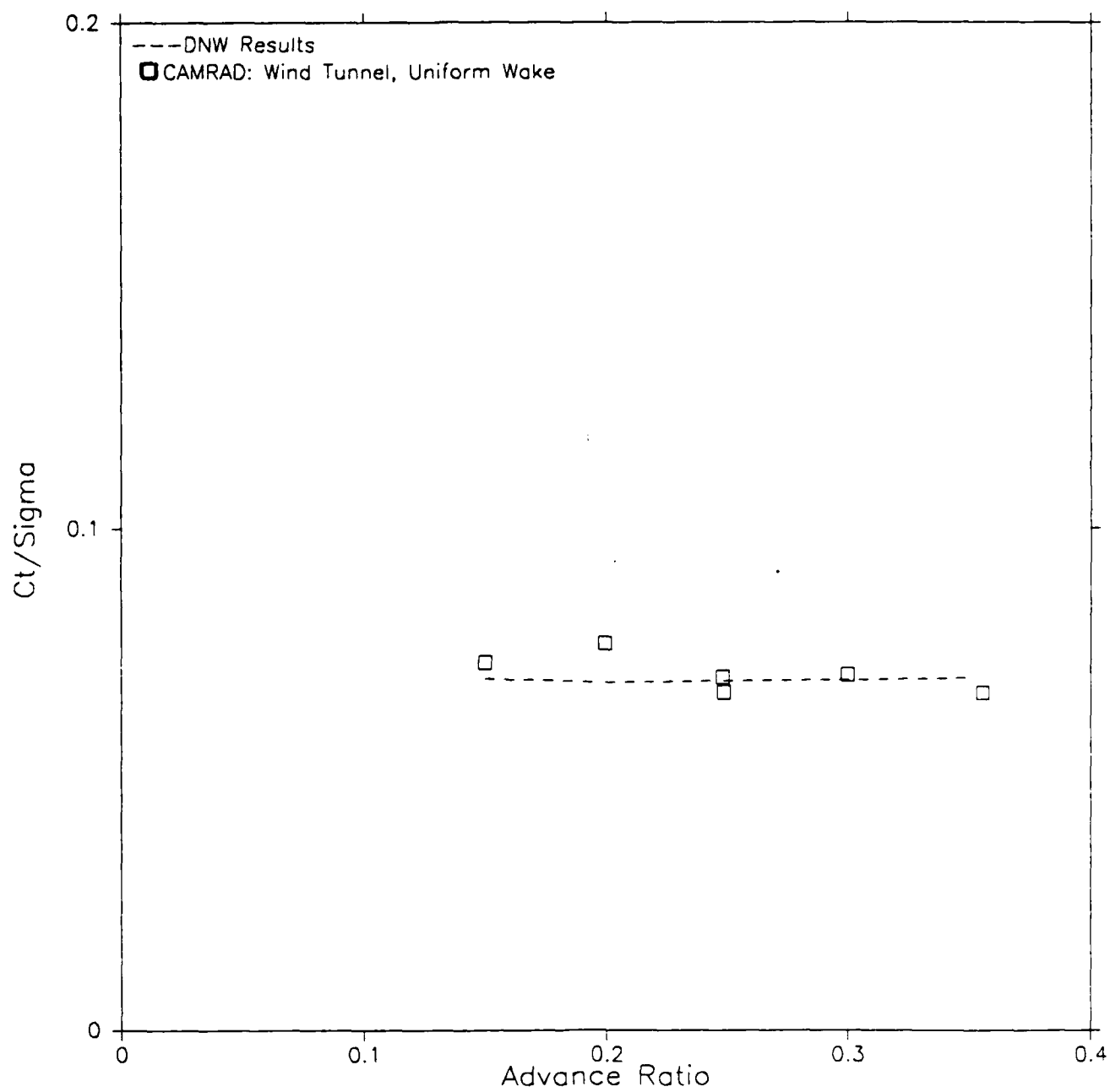
FIGURE 12 : Thrust Coefficient vs Shaft Angle

---DNW Results
□CAMRAD: Wind Tunnel, Uniform Wake
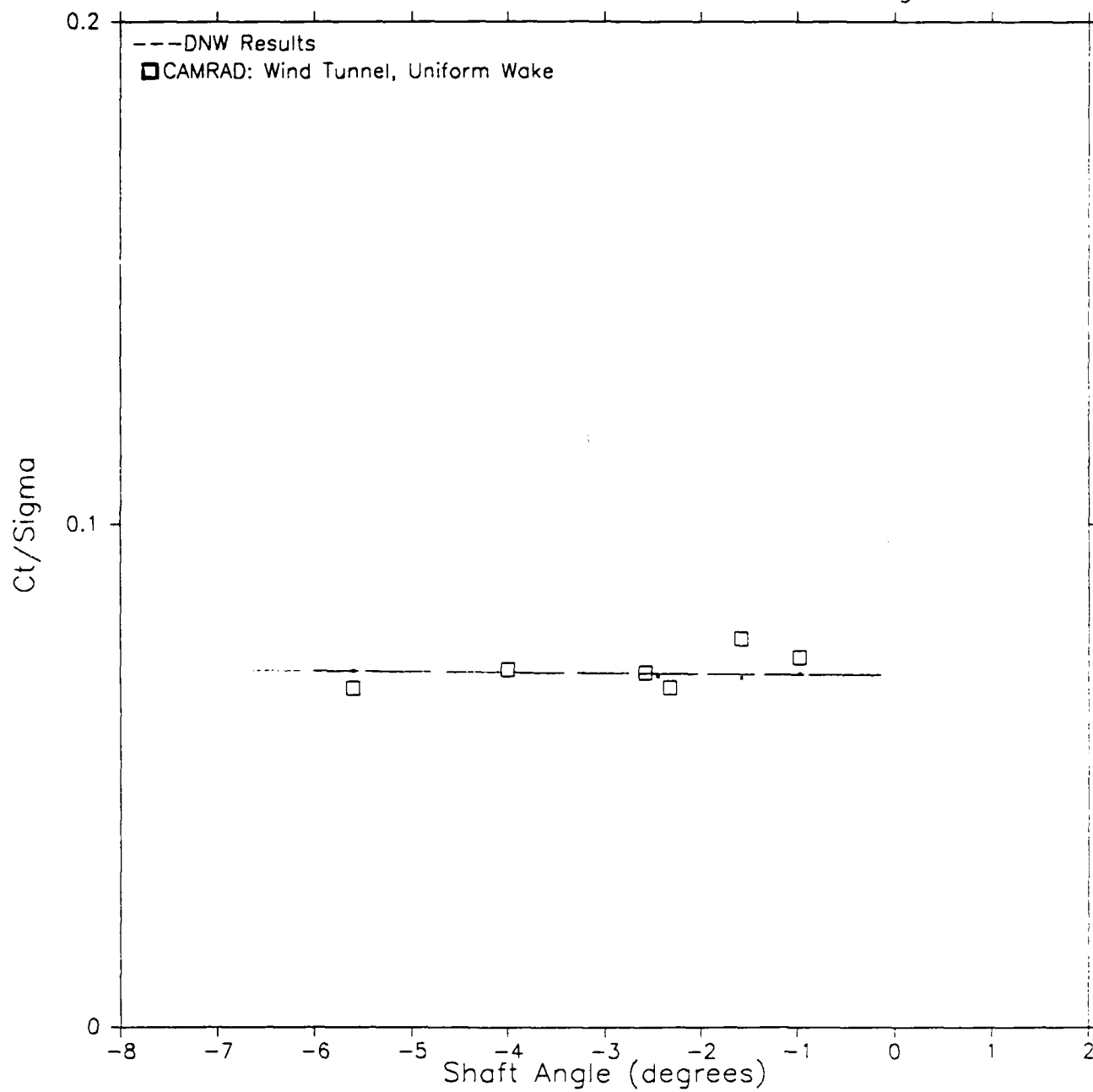
FIGURE 13: Propulsive Coefficient vs Advance Ratio
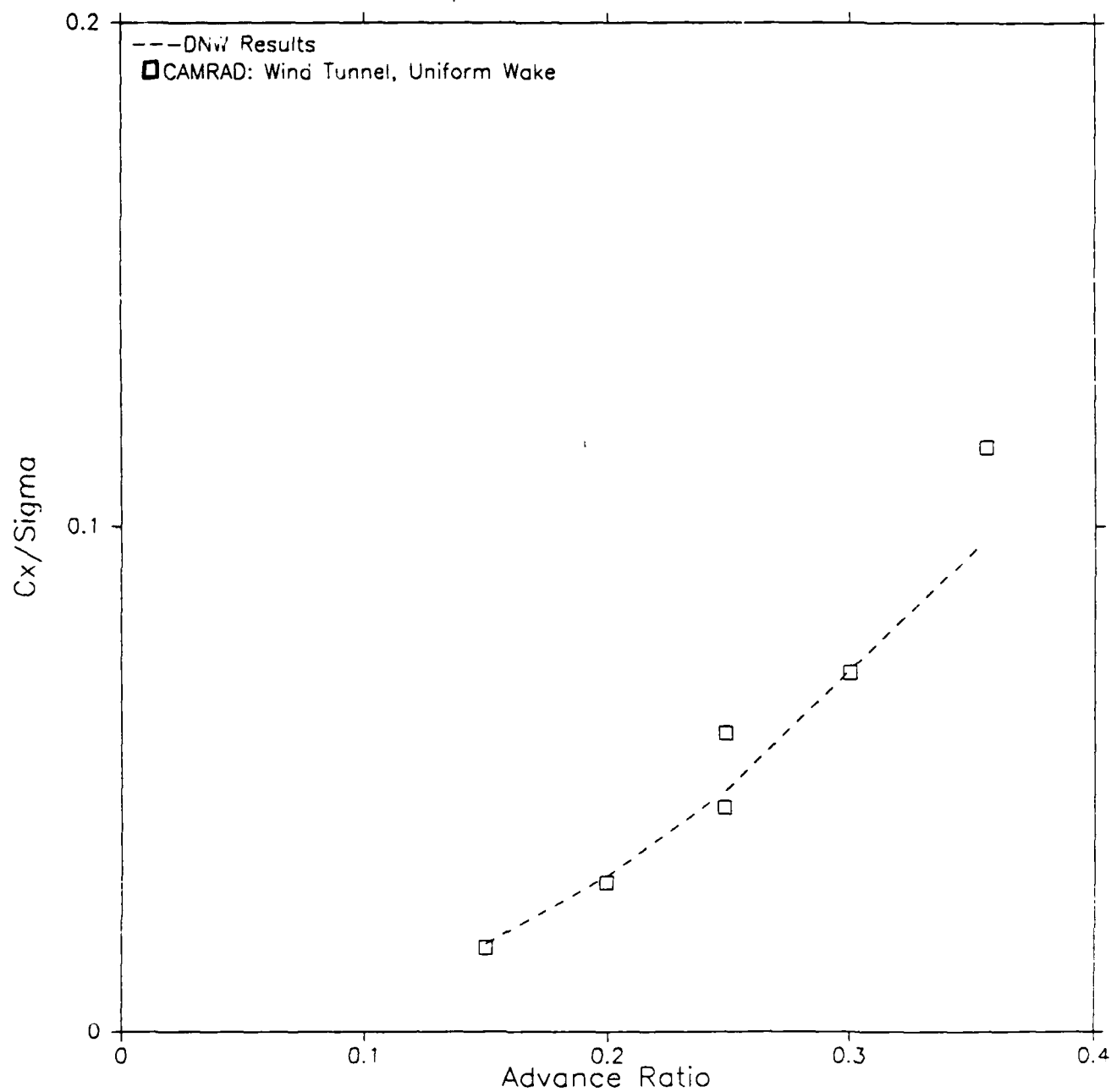
FIGURE 14 : Propulsive Coefficient vs Shaft Angle
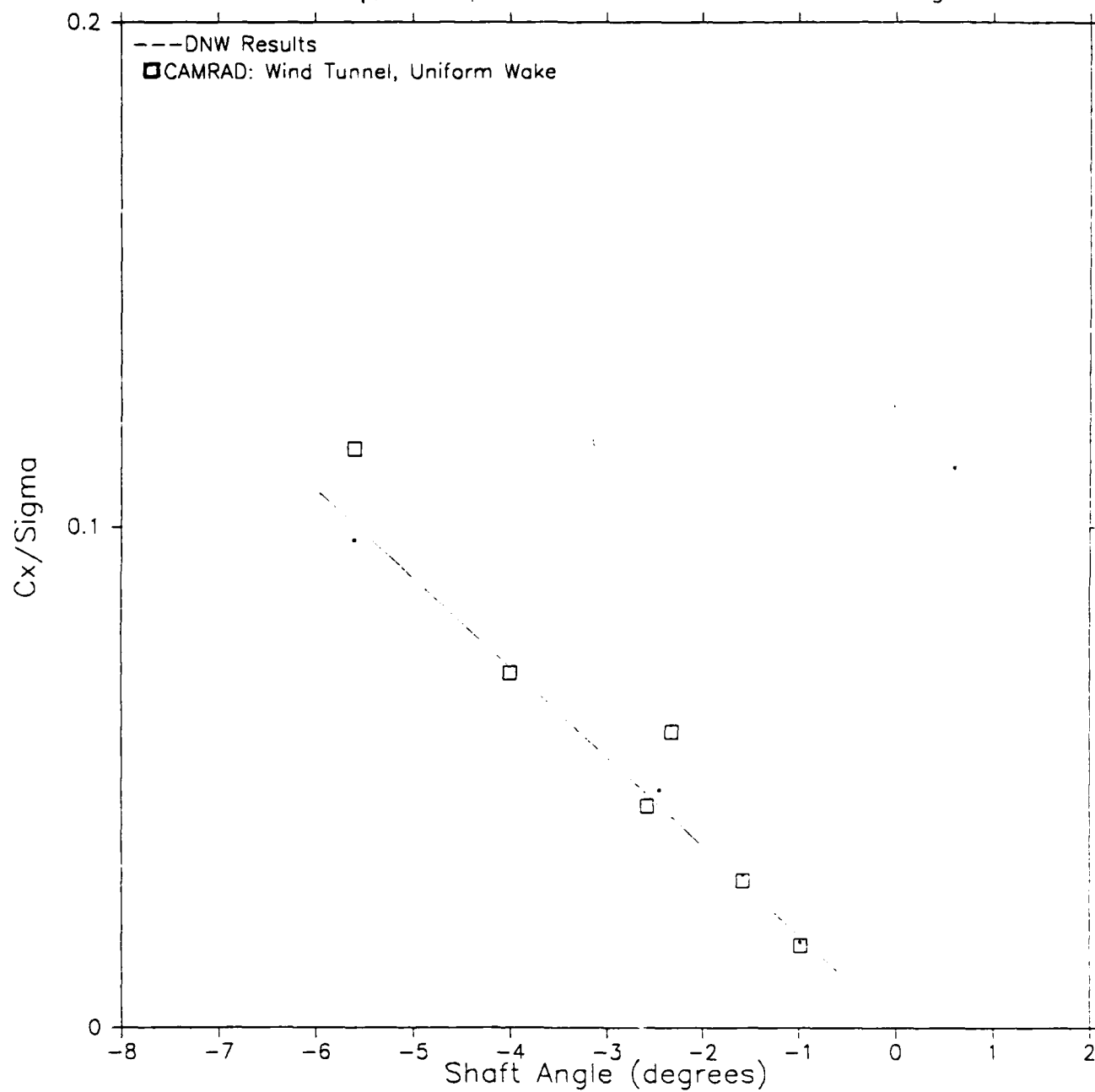
FIGURE 15: Collective vs Advance Ratio
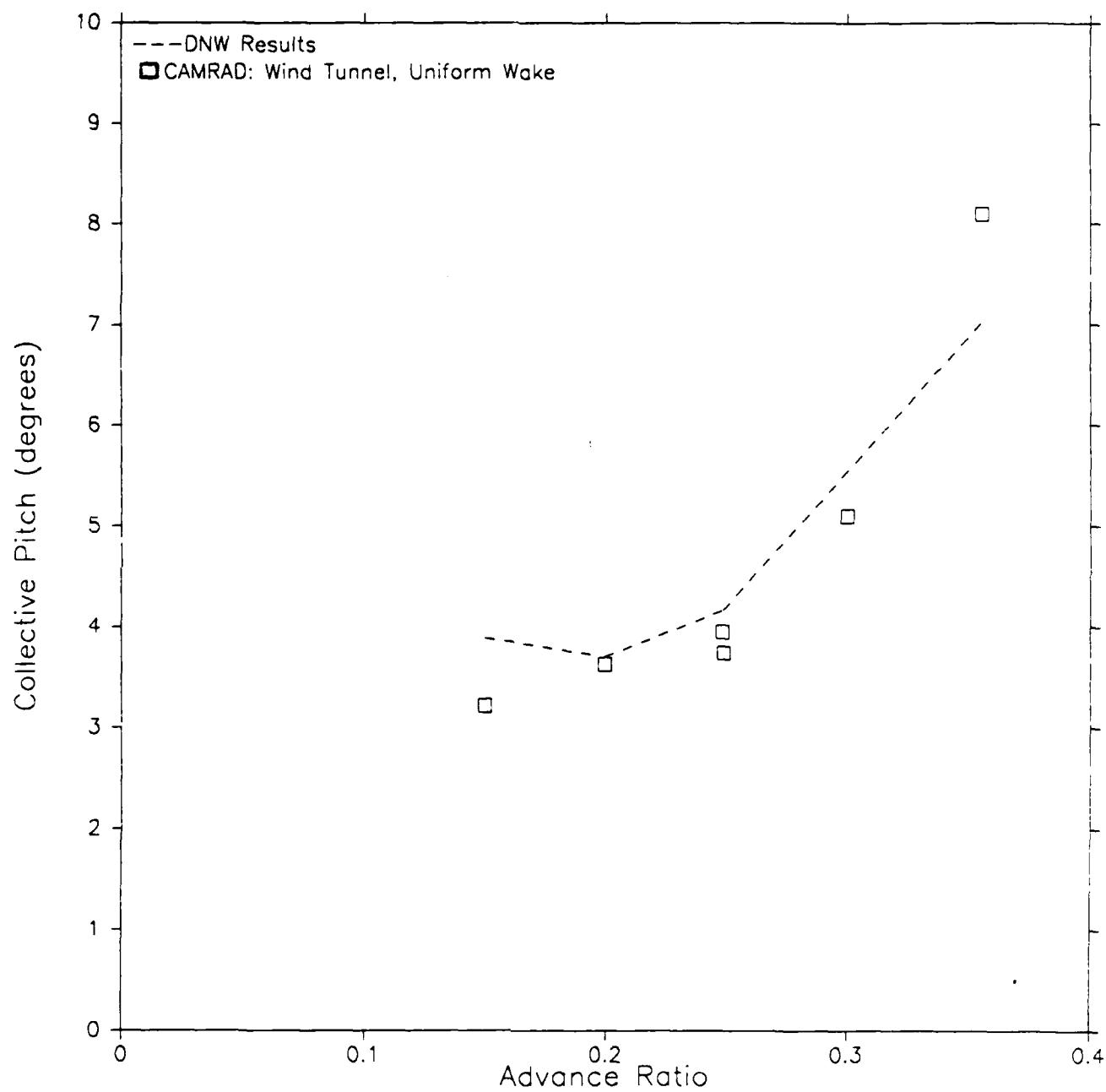
FIGURE 16: Lateral Cyclic vs Advance Ratio
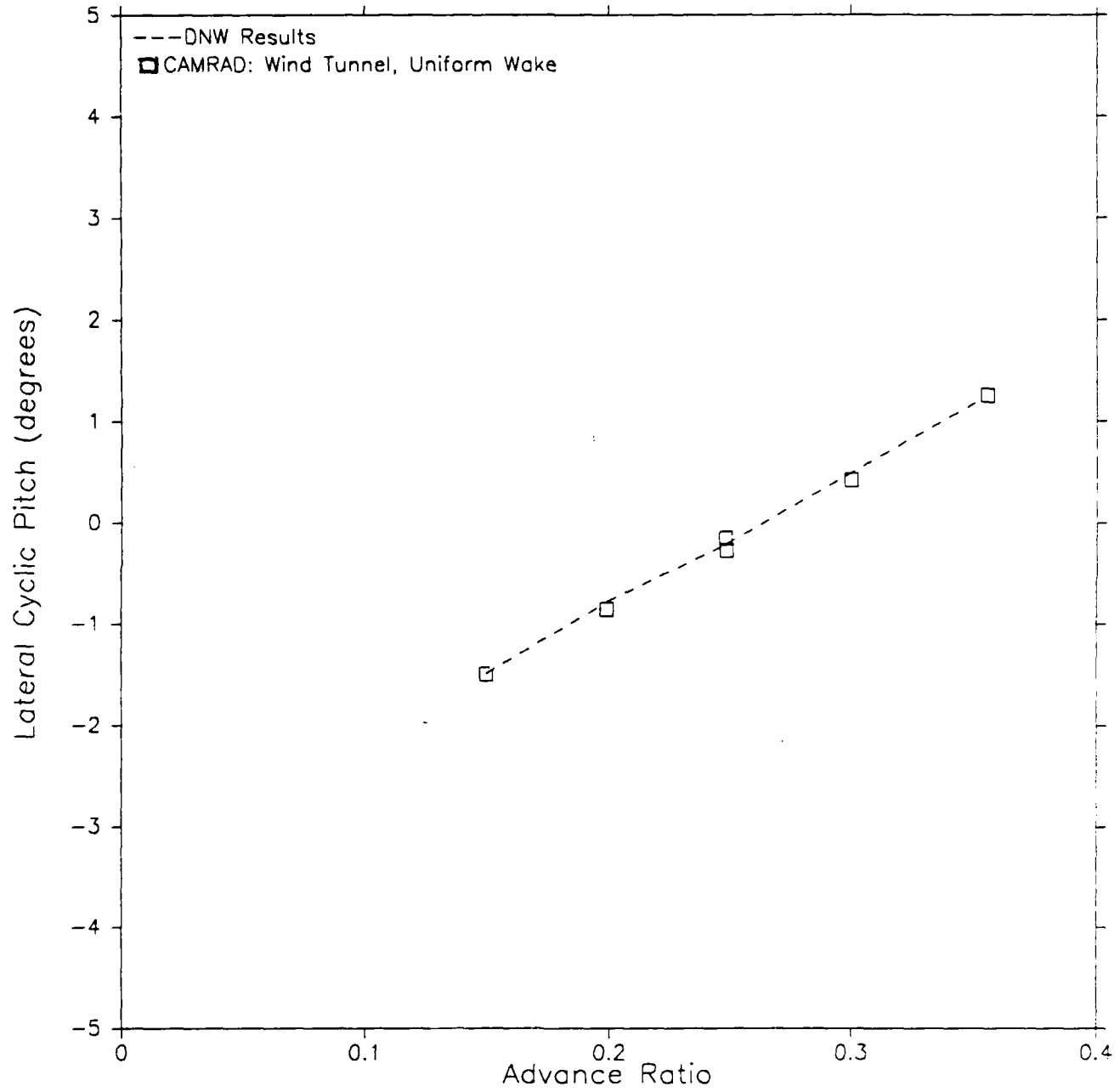
FIGURE 17: Longitudinal Cyclic vs Advance Ratio

FIG 18: Wake Geometry at Advance Ratio=0.15
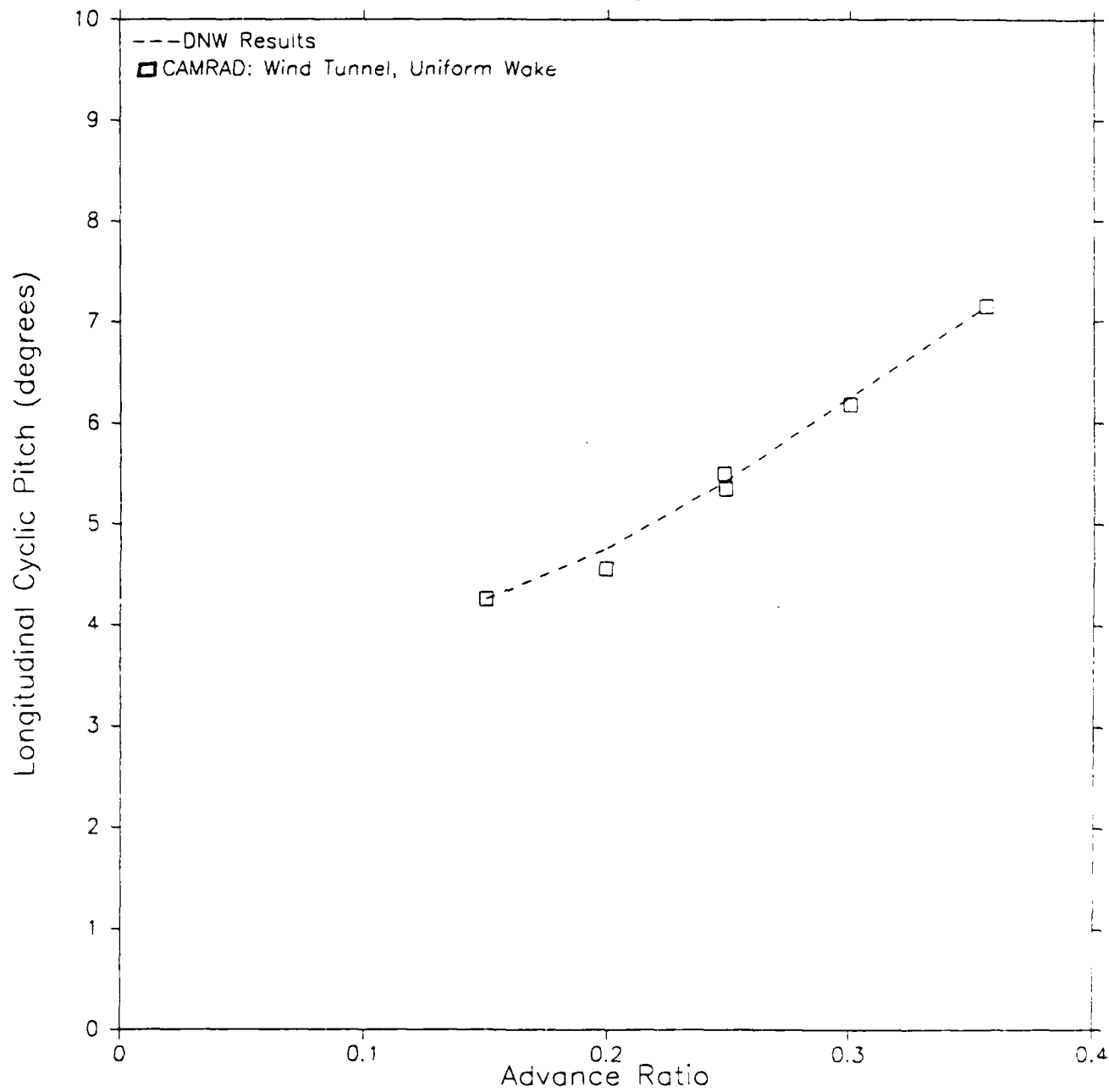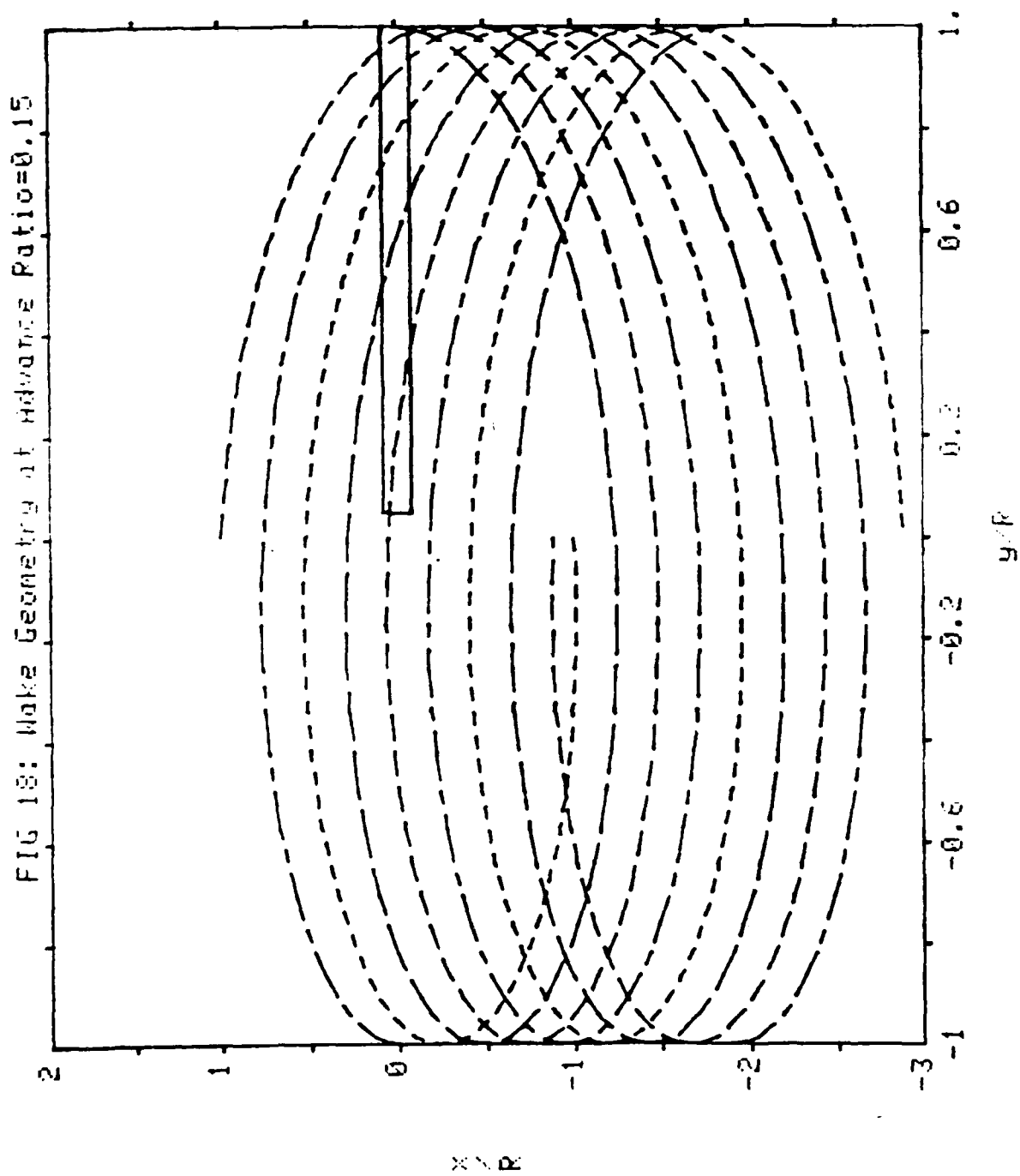
FIG 19: Wake Geometry at Advance Ratio=0.15
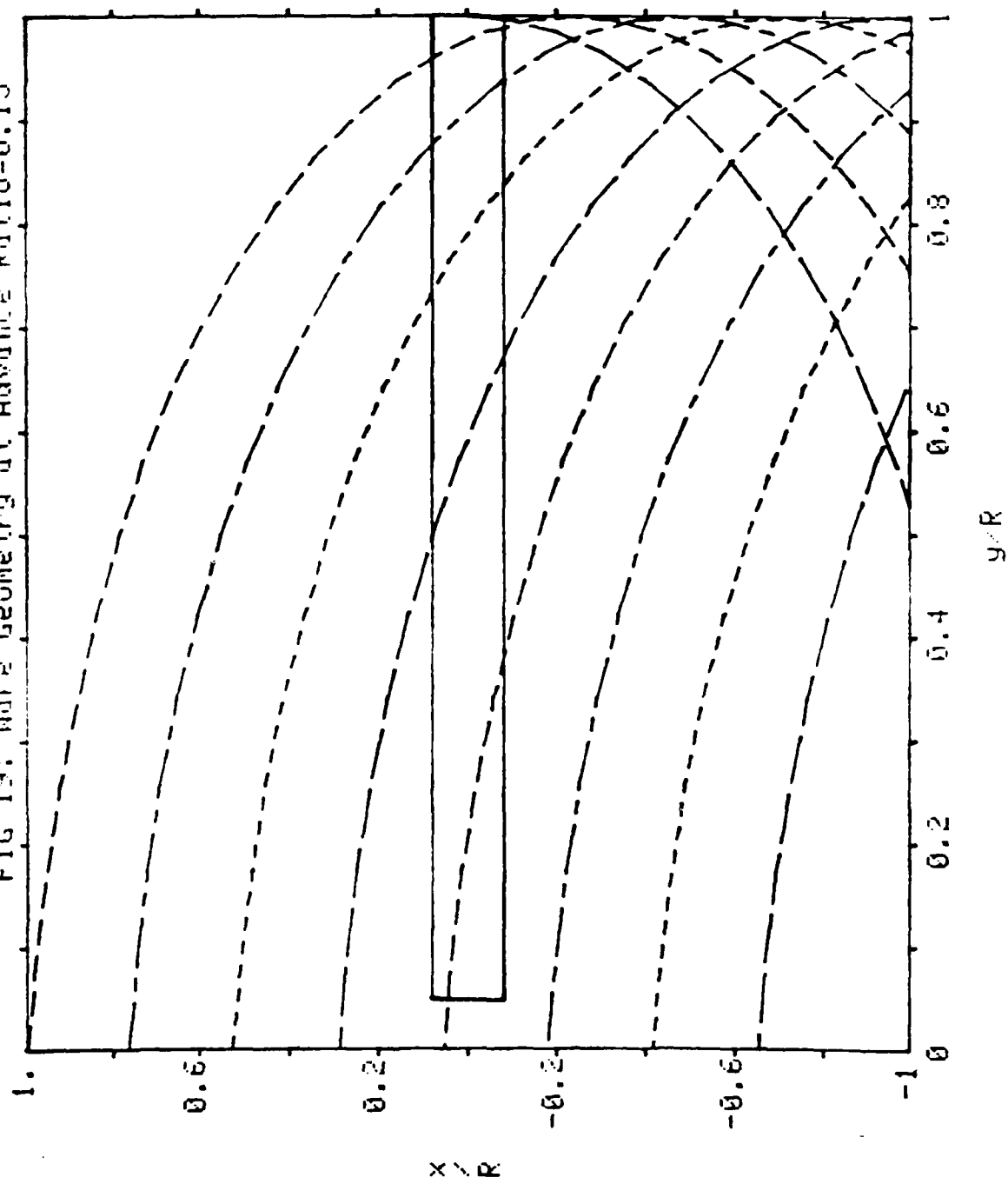
FIGURE 20: Thrust Coefficient vs Advance Ratio
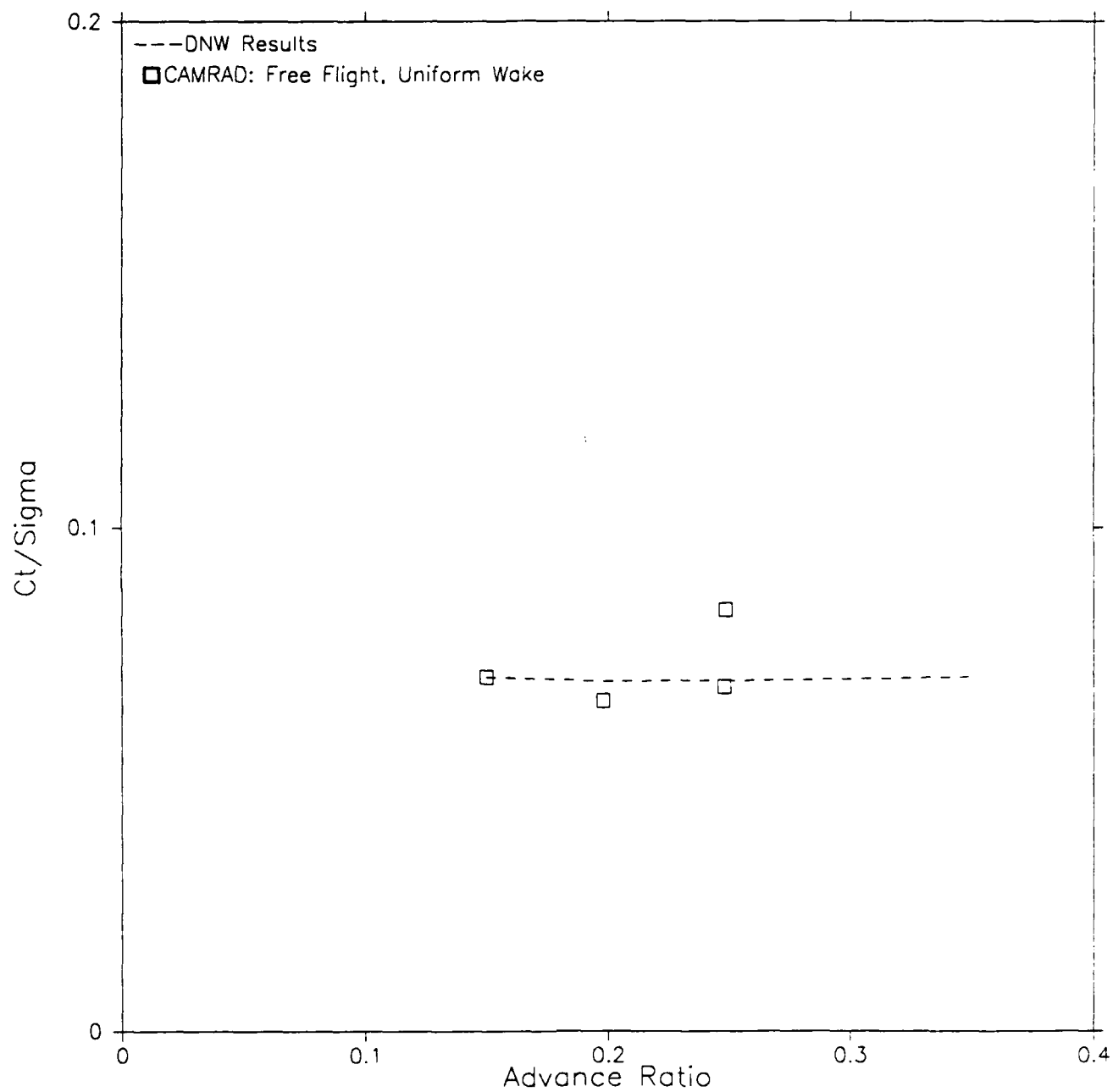
FIGURE 21: Propulsive Coefficient vs Advance Ratio
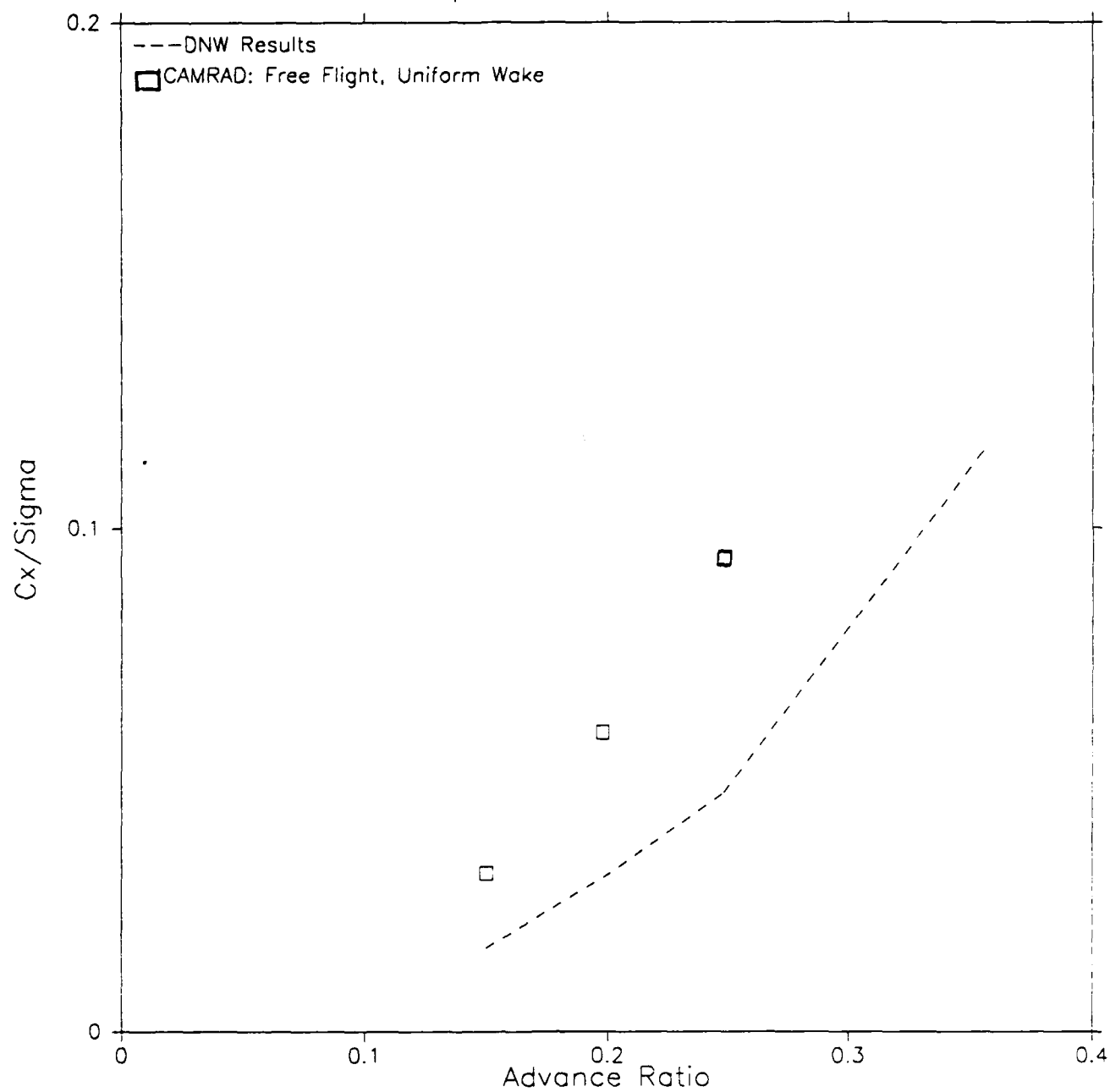
FIGURE 22: Lift Coefficient vs Azimuth Angle
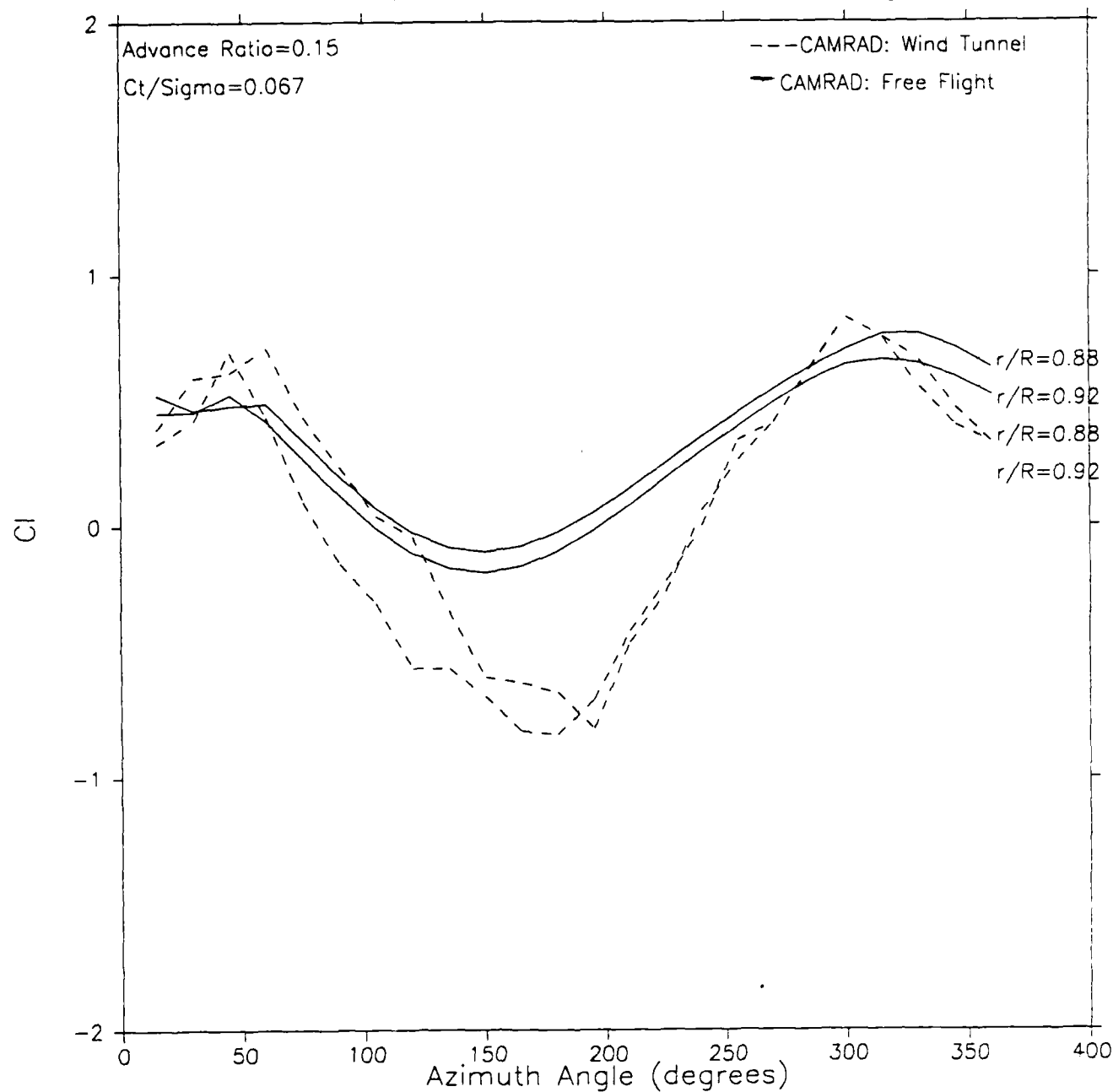
FIGURE 23: Lift Coefficient vs Azimuth Angle
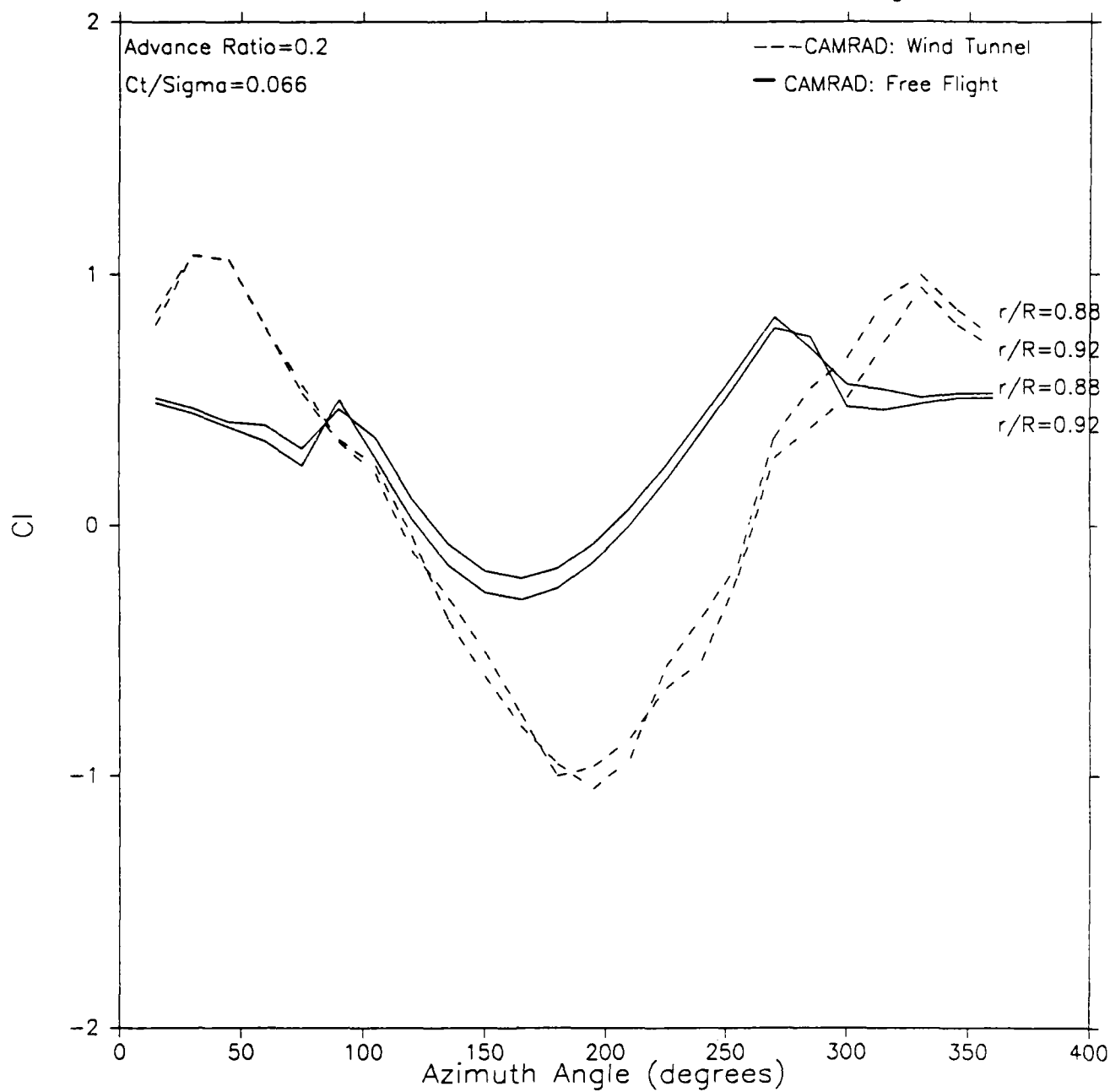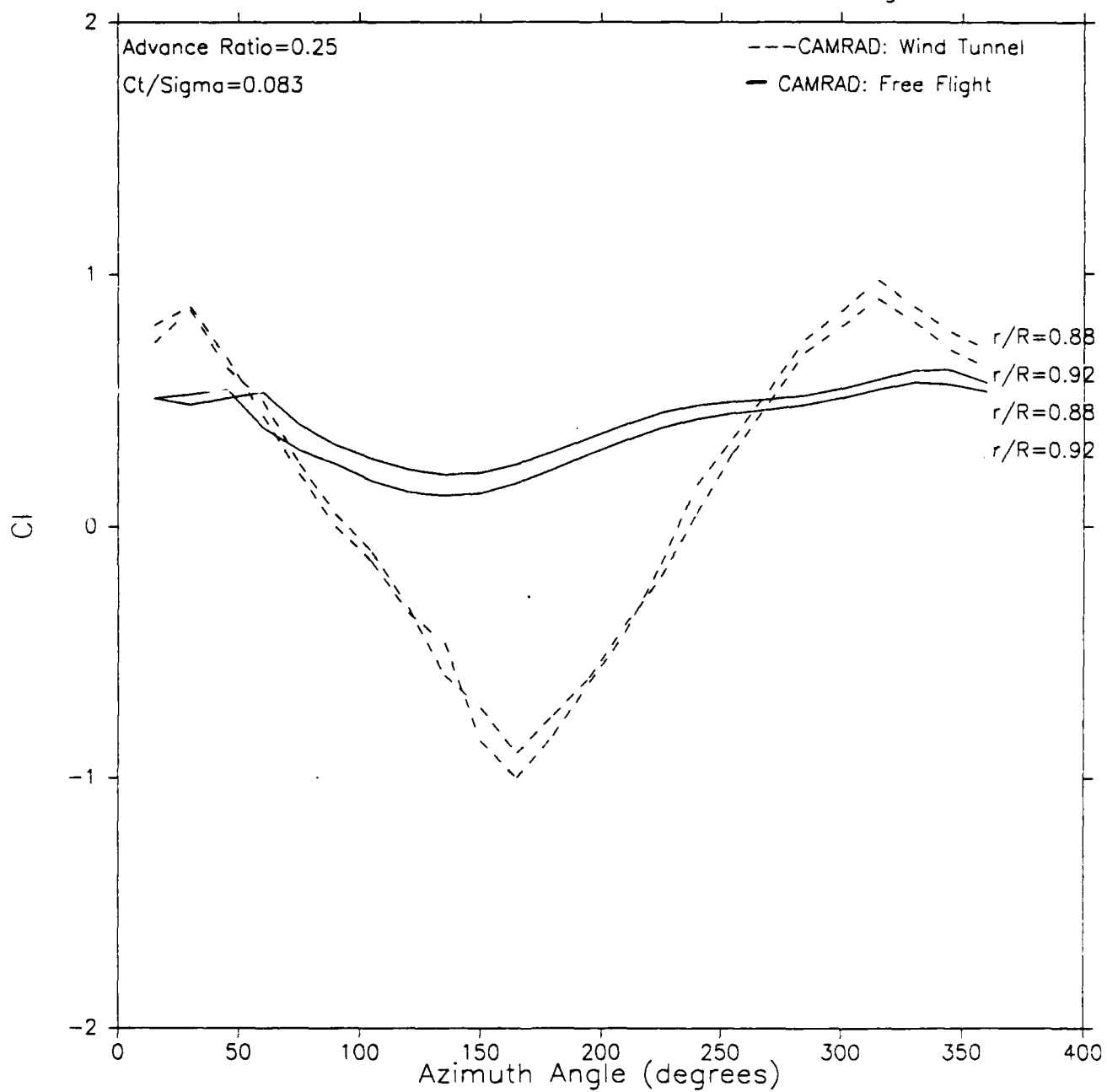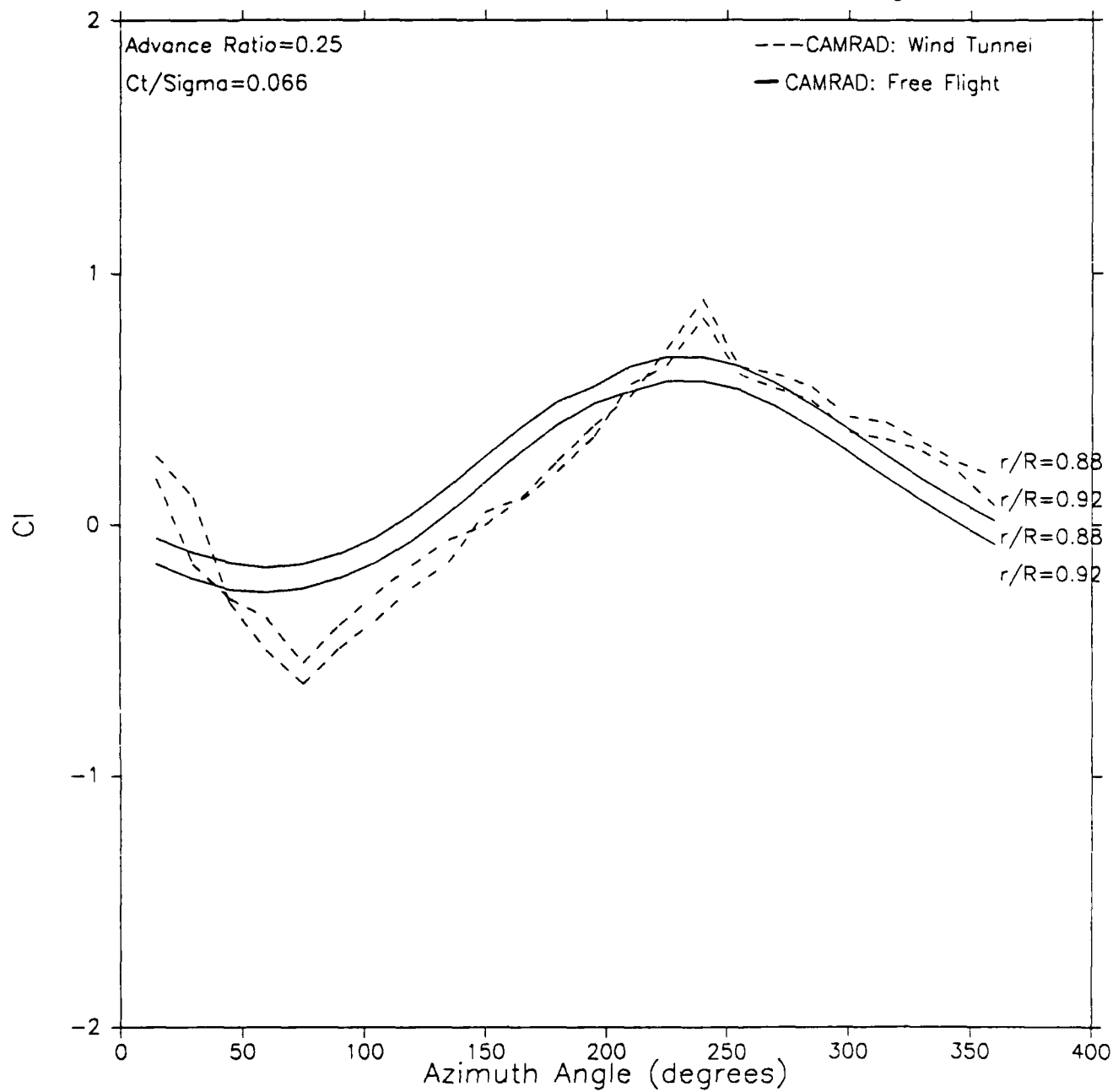
FIGURE 24: Lift Coefficient vs Azimuth Angle

Advance Ratio=0.25
Ct/Sigma=0.083

- - - CAMRAD: Wind Tunnel
—— CAMRAD: Free Flight

r/R=0.88
r/R=0.92
r/R=0.88
r/R=0.92

Cl

Azimuth Angle (degrees)

FIGURE 25: Lift Coefficient vs Azimuth Angle
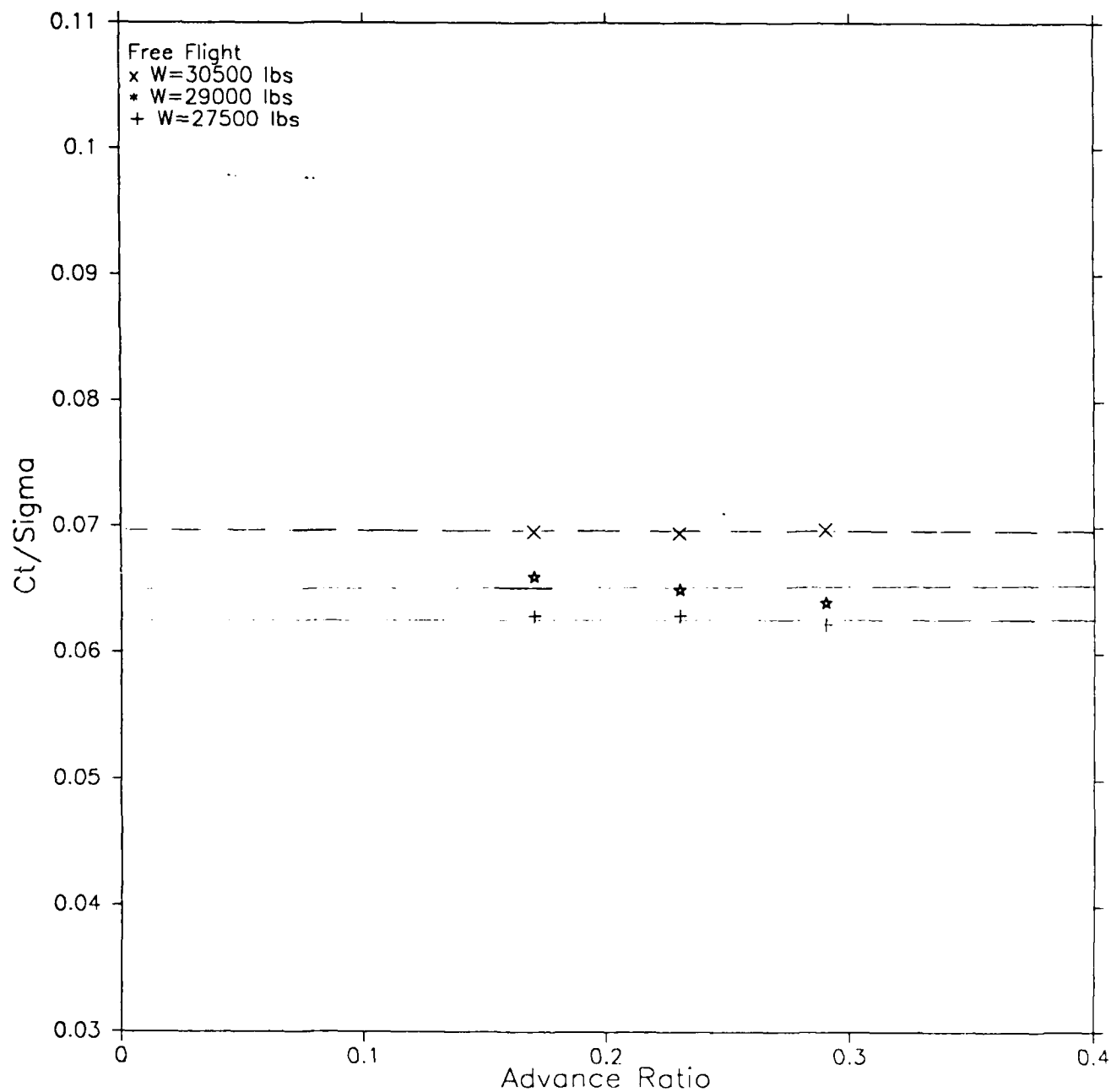
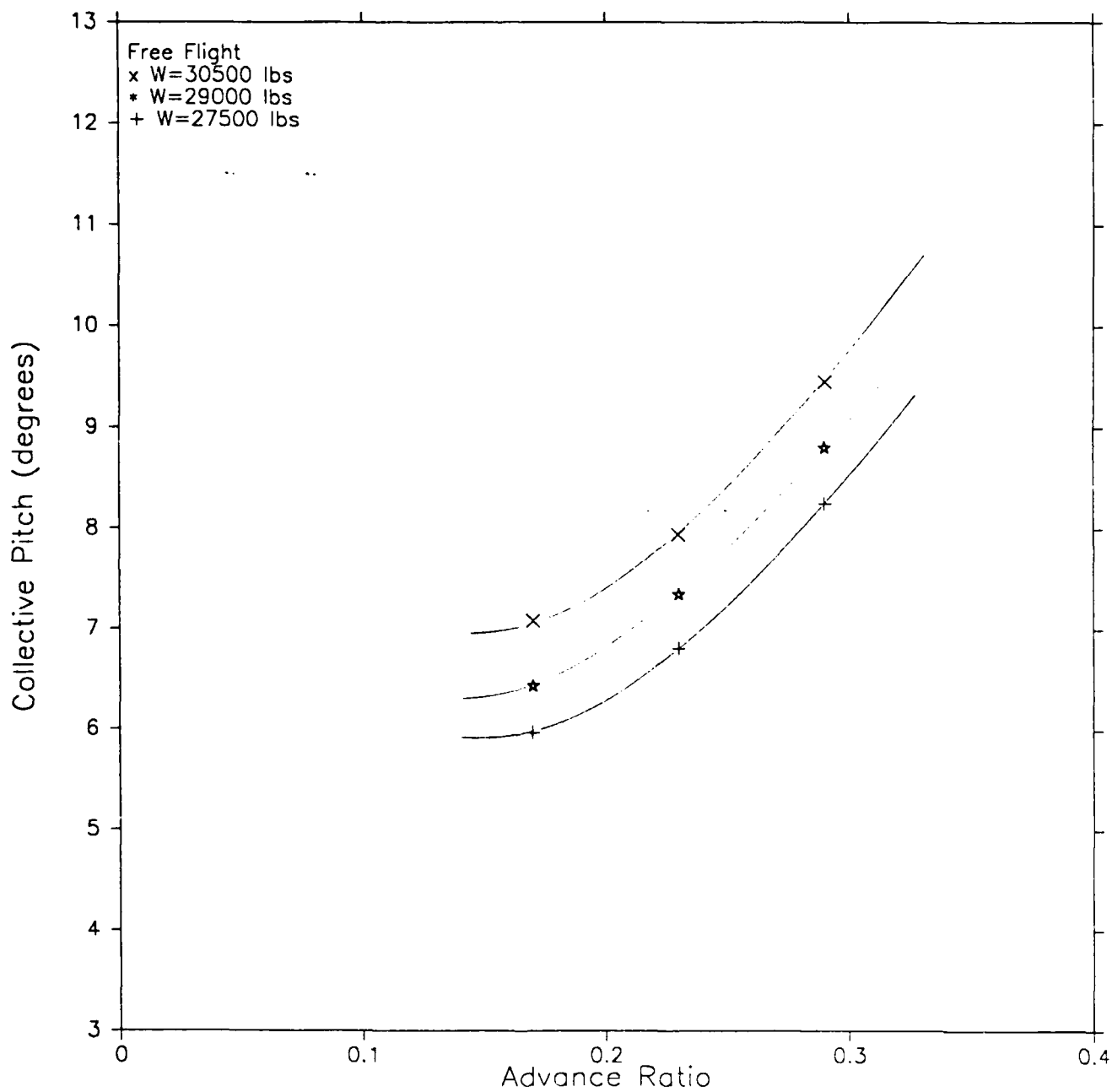FIGURE 26 : Thrust Coefficient vs Advance Ratio

FIGURE 27: Collective vs Advance Ratio

FIGURE 28 : Lateral Cyclic vs Advance Ratio